New remains of kollpaniine "condylarths" (Panameriungulata) from the early Palaeocene of Bolivia shed light on hypocone origins and molar proportions among ungulate-like placentals

Christian de Muizon, Guillaume Billet, Sandrine Ladevèze

geodiversitas

2019 • 41 • 25

New remains of kollpaniine “condylarths” (Panameriungulata) from the early Palaeocene of Bolivia shed light on hypocone origins and molar proportions among ungulate-like placentals

Christian de MUIZON, Guillaume BILLET & Sandrine LADEVÈZE

art. 41 (25) — Published on 19 December 2019
www.geodiversitas.com

MUSÉUM NATIONAL D'HISTOIRE NATURELLE
PUBLICATIONS SCIENTIFIQUES

Geodiversitas est indexé dans / Geodiversitas *is indexed in:*
– Science Citation Index Expanded (SciSearch®)
– ISI Alerting Services®
– Current Contents® / Physical, Chemical, and Earth Sciences®
– Scopus®

Geodiversitas est distribué en version électronique par / Geodiversitas *is distributed electronically by:*
– BioOne® (http://www.bioone.org)

Les articles ainsi que les nouveautés nomenclaturales publiés dans *Geodiversitas* sont référencés par / *Articles and nomenclatural novelties published in* Geodiversitas *are referenced by:*
– ZooBank® (http://zoobank.org)

Geodiversitas est une revue en flux continu publiée par les Publications scientifiques du Muséum, Paris
Geodiversitas *is a fast track journal published by the Museum Science Press, Paris*

Les Publications scientifiques du Muséum publient aussi / *The Museum Science Press also publish:*
Adansonia, ***Zoosystema***, ***Anthropozoologica***, ***European Journal of Taxonomy***, ***Naturae***, ***Cryptogamie*** **sous-sections** ***Algologie***, ***Bryologie***, ***Mycologie.***

Diffusion – Publications scientifiques Muséum national d'Histoire naturelle
CP 41 – 57 rue Cuvier F-75231 Paris cedex 05 (France)
Tél. : 33 (0)1 40 79 48 05 / Fax : 33 (0)1 40 79 38 40
diff.pub@mnhn.fr / http://sciencepress.mnhn.fr

ISSN (imprimé / *print*) : 1280-9659/ ISSN (électronique / *electronic*) : 1638-9395

New remains of kollpaniine “condylarths” (Panameriungulata) from the early Palaeocene of Bolivia shed light on hypocone origins and molar proportions among ungulate-like placentals

Christian de MUIZON
Guillaume BILLET
Sandrine LADEVÈZE
CR2P (CNRS, MNHN, Sorbonne Université),
Département Origines et Évolution, Muséum national d’Histoire naturelle,
case postale 38, 57 rue Cuvier, F-75231 Paris cedex 05 (France)

Submitted on 26 February 2019 | accepted on 27 June 2019 | published on 19 December 2019

urn:lsid:zoobank.org:pub:4EF01B8A-BA1D-4F14-9432-CA8754D765D2

Muizon C. de, Billet G. & Ladevèze S. 2019. — New remains of kollpaniine “condylarths” (Panameriungulata) from the early Palaeocene of Bolivia shed light on hypocone origins and molar proportions among ungulate-like placentals. *Geodiversitas* 41 (25): 841-874. https://doi.org/10.5252/geodiversitas2019v41a25. http://geodiversitas.com/41/25

ABSTRACT
The description of new specimens of kollpaniines “condylarths” from Tiupampa (early Palaeocene of Bolivia) represents a significant addition to the knowledge of the earliest fauna of South American ungulates. Several partial mandibles and maxillae of *Molinodus suarezi* and *Simoclaenus sylvaticus* are described. The morphology of the lower premolars of *Molinodus*, being associated to lower molars, is established and a previous referral of an isolated p4 is rejected. A maxilla of *Simoclaenus* reveals the morphology of the so far unknown P1-4 of this taxon and allows a discussion on the development of the protocone in Palaeocene “condylarths”. The subvertical maxilla-premaxilla suture and the vertical implantation of the P1/p1 confirm the shortness of the snout of *Simoclaenus*, whereas the procumbency of the p1 of *Molinodus* indicates a longer rostrum. The upper molars of *Molinodus* confirm the presence of a tendency to duplication of the protocone, which is regarded as the incipient development of a pseudohypocone. The various patterns of formation of a hypocone (or pseudohypocone) are considered and, among other South American Native Ungulates, a protocone-derived pseudohypocone (i.e. *Molinodus*-like) is hypothesized in *Lamegoia, Raulvaccia,* and notoungulates, whereas a postcingulum-derived, hypocone is present in didolodontids and litopterns.

The new specimens confirm the conspicuous small size of the M1/m1 of *Molinodus* and *Simoclaenus* as compared to the M2/m2. Consequently, we examined the relative proportions of molars in these taxa as compared to a variety of extant and extinct euungulates. Their proportions were plotted into the ‘developmental’ morphospace based on the predictive mathematical model of Kavanagh *et al.* (2007) (Inhibitory Cascade Model, or IC model), which might explain a large part of the mammalian diversity in molar proportions. Based on the upper molars, the Tiupampa kollpaniines were retrieved in a separate area of the predicted morphospace with other North American “condylarths” with large M2; this departure is also consistent with previous results concerning the lower molars (large m2). These peculiar molar proportions were found distinct from many other mammals, and might represent clade-specific differences: the large size of both the upper and lower second molars relative to other molars thus possibly representing a derived character state shared by some “condylarths” and kollpaniines.

KEY WORDS
Kollpaniinae,
“condylarths”,
early Palaeocene,
Bolivia,
hypocone,
pseudohypocone,
molars relative
proportions.

RÉSUMÉ
De nouveaux restes de « condylarthres » kollpaniinés (Panameriungulata) du Paléocène inférieur de Bolivie contribuent à l'interprétation des origines de l'hypocone et des proportions des molaires chez les placentaires à morphologie d'ongulés.
La description de nouveaux spécimens de « condylarthres » kollpaniinés de Tiupampa (Paléocène inférieur de Bolivie) constitue un complément d'information significatif à la connaissance de la plus ancienne faune d'ongulés sud-américains. Plusieurs mandibules et maxillaires partiels de *Molinodus suarezi* et *Simoclaenus sylvaticus* sont décrits. La morphologie des prémolaires inférieures de *Molinodus*, étant associées à des molaires, est établie et l'attribution antérieure d'une p4 isolée à ce taxon est rejetée. Un maxillaire de *Simoclaenus* révèle la morphologie, inconnue auparavant, des P1-4 de ce taxon et permet une discussion sur le développement du protocone des prémolaires chez des « condylarthres » du Paléocène. La suture maxillaire-prémaxillaire, subverticale, et l'implantation verticale des P1/p1 confirme la faible longueur du museau de *Simoclaenus*, tandis que la p1 de *Molinodus*, légèrement proclive, indique un rostre plus long. Les molaires supérieures de *Molinodus* confirment la présence d'une tendance la duplication du protocone qui est considérée comme le développement initial d'un pseudohypocone. Les modalités de formation d'un hypocone (ou pseudohypocone) sont considérées et, parmi les autres ongulés natifs sud-américains, l'hypothèse de la formation d'un pseudohypocone, dérivé du protocone (de type *Molinodus*), est proposée chez *Lamegoia*, *Raulvaccia* et les notongulés, tandis qu'un vrai hypocone, dérivé du postcingulum, est présent chez les didolodontes et les litopternes.

Les nouveaux spécimens confirment la petite taille des M1/m1 de *Molinodus* et *Simoclaenus* par rapport aux M2/m2. Les proportions relatives des molaires ont donc été examinées chez ces taxons et comparées à plusieurs euongulés actuels et fossiles. Leurs proportions ont été reportées sur un graphe dans l'espace morphologique de développement fondé sur le modèle mathématique prédictif de Kavanagh *et al.* (2007) (Inhibitory Cascade Model), qui pourrait expliquer une grande partie de la diversité des proportions des molaires de mammifères. Sur la base des molaires supérieures, les kollpaniinés de Tiupampa se situent dans une aire séparée de l'espace morphologique prédit, et ce, avec d'autres « condylarthres » nord-américains (possédant une grande M2). Cet écart est consistant avec les résultats antérieurs concernant les molaires inférieures (grandes m2). Ces proportions particulières sont différentes de celles de nombreux autres mammifères et pourrait représenter une spécificité de clade concernant les tailles relatives des molaires : la grande taille des deuxièmes molaires supérieures et inférieures pourrait donc constituer un caractère dérivé partagé par certains « condylarthres » et les kollpaniinés.

MOT CLÉS
Kollpaniinae,
« condylarthres »,
Paléocène inférieur,
Bolivie,
protocone des
prémolaires,
hypocone,
pseudohypocone,
proportions relatives
des molaires.

INTRODUCTION

The locality of Tiupampa (Cochabamba, Bolivia) has yielded the oldest mammalian assemblage of the Cenozoic of South America and is the type locality of the Tiupampan South America Land Mammal Age (SALMA), (Gelfo *et al.* 2009). The only possibly older Cenozoic mammal of South America is an isolated lower molar of polydolopimorphian (*Cocatherium lefipanum*) from the Lefipan Formation at the Grenier farm (Chubut, Argentina) and discovered in beds located about 5 m above the K-T boundary (Goin *et al.* 2006). A recent revision of Palaeogene SALMAs agreed with this view and considered a 64 Ma age for the Tiupampan (Woodburne *et al.* 2014a). The age of the Tiupampan has been reconsidered more recently and is regarded as closer to 65 Ma (early Danian), (Muizon *et al.* 2015, 2018). The Tiupampa mammals have been recovered from beds regarded as belonging to the chron 28r (Marshall *et al.* 1997; Gelfo *et al.* 2009), which, according to Wilson (2013, 2014) and Sprain *et al.* (2015), is bracketed between *c.* 65 Ma and 64.866 Ma. It is regarded as an equivalent of the earliest Torrejonian 1 of North America.

The Tiupampa fauna includes only eutherians and metatherians, both of which are taxonomically abundant (12 metatherians and 11 eutherians). Some taxa are exceptionally well represented by partial to sub-complete skulls and skeletons. Among eutherians the pantodont *Alcidedorbignya inopinata* is the most abundant taxon and is known by three adult skulls, one of them being associated to an almost complete skeleton (Muizon *et al.* 2015). However, the most diverse eutherians at Tiupampa are the "condylarths". "Condylarthra" is currently viewed as "an assortment of ungulategrade Palaeogene mammals" (Shelley *et al.* 2018: 2) and therefore probably polyphyletic (e.g., Halliday *et al.* 2017). The Tiupampa "condylarths" are represented by five genera and seven species, which are included in the same, so far endemic, sub-family of Mioclaenidae, the Kollpaniinae (Muizon & Cifelli 2000). The five genera of Kollpaniinae have a very similar morphological pattern and constitute a monophyletic taxon in most phylogenetic hypotheses (Muizon & Cifelli 2000; Gelfo 2007; Gelfo & Sigé 2011). Kollpaniinae have not been discovered in other localities of South America yet, but it is noteworthy that Tiupampan beds have not been identified elsewhere than in Tiupampa

either. The oldest Cenozoic mammalian fauna in South America after that of Tiupampa is that of Punta Peligro (Argentina), which has been regarded as late Palaeocene in age (Peligran = early Selandian, *c.* 61 Ma, Woodburne *et al.* 2014a). However, Woodburne *et al.* 2014b and Clyde *et al.* (2014) refer the Punta Peligro fauna to the late Danian with an age of *c.* 63.5 Ma. So far, no kollpaniine "condylarths" have been recovered at Punta Peligro. One single tooth outside Tiupampa has been referred to the Mioclaenidae and, as such, bears similarities with the Kollpaniinae. This specimen is the holotype of *Pascualodus patagoniensis* and is from the late Casamayoran (Barrancan = Bartonian) of Patagonia Argentina (*c.* 40 Ma) (Gelfo 2004). Therefore, in the present state of our knowledge, the Tiupampa "condylarth" fauna, taxonomically diverse at generic level (5 taxa) but very homogeneous at subfamilial level (Kollpaniinae), represents the oldest known evidence of the ungulate-like placentals radiation in South America. Kollpaniines, which are potentially related to litopterns (Muizon & Cifelli 2000), may in fact document one of the first steps of the diversification of South American Native Ungulates (SANUs) on this continent. Recent proteomic and mitogenomic data showed that litopterns and notoungulates are closely related to the Perissodactyla (Welker *et al.* 2015; Buckley 2015; Westbury *et al.* 2017), an order of mammals still represented today and probably originating from northern continents (Cooper *et al.* 2014; Rose *et al.* 2014; Bai *et al.* 2018). According to these hypotheses, the Notoungulata and Litopterna would thus also belong to the Euungulata together with the Perissodactyla and Artiodactyla (Asher & Helgen 2010). The divergence between Litopterna and Perissodactyla was estimated close to 66 Ma (Westbury *et al.* 2017), which confers considerable importance to the fossil kollpaniines from Tiupampa (estimated *c.* 65 Ma) to further disentangle the phylogenetic and spatiotemporal aspects of this divergence.

However, the fossil remains of Tiupampa kollpaniines, although relatively abundant, are not as well preserved as those of *Alcidedorbignya* since they are only represented by isolated jaws and some postcranial elements, which are most of the time, not associated. Therefore, the fossil record of the Kollpaniinae is relatively incomplete and any new specimen is susceptible to improve substantially the knowledge of this group. Since the description of the Tiupampa kollpaniine fauna (Muizon & Cifelli 2000), several field expeditions have been undertaken at Tiupampa, which have unearthed some interesting new kollpaniine specimens. Here, we describe these new specimens with an aim at providing critical anatomical information on this early diversification and on potential phylogenetic relationships to other "condylarths" and to SANUs. The description of these remains also involves considerations on the hypocone formation within these groups and a comparison of the peculiar molar proportions found in kollpanines with other "condylarths" and ungulate or ungulate-like mammals within the frame of recently developed evo-devo models on this aspect (Kavanagh *et al.* 2007; Polly 2007).

MATERIAL AND METHODS

In this paper, we intend to describe the most relevant new specimens of kollpaniines collected at Tiupampa, which are referred to five species belonging to four genera, *Molinodus suarezi*, *Simoclaenus sylvaticus*, *Tiuclaenus minutus*, *Tiuclaenus robustus*, and *Pucanodus gagnieri*. No new specimens of *Andinodus boliviensis* have been recovered, and, so far, the only known specimens of this taxa are the two lower jaw fragments described by Muizon & Cifelli (2000).

The most abundant kollpaniine taxon at Tiupampa is *Molinodus suarezi*. Three partial mandibles respectively with p3-m3 (MHNC 13867), m2-3, (MHNC 13871) and c-p1 (MHNC 13883), and one left partial maxilla with M1-3 (MHNC 13870) substantially increment the knowledge of the dental anatomy of this taxon. *Simoclaenus sylvaticus* is a relatively rare taxon at Tiupampa and was up to now only known from two specimens, the holotype, a partial mandible with p4-m3, and a partial maxilla with M1-3. The new specimens of *S. sylvaticus* are a partial maxilla with the root of the canine and P1-4 (MHNC 13868), a partial maxilla with M1-2 (MHNC 13876), and a partial mandible with roots of p2-3 and p4-m1 (MHNC 13872). A partial maxilla with M1-3 (MHNC 13879), is referred to *Tiuclaenus minutus* and a partial mandible with m2-3 (MHNC 13875) is referred to *T. robustus*. A partial mandible with almost unworn m2-3 (MHNC 13869) is referred to *Pucanodus gagnieri*. The other specimens are either poorly preserved or not informative as compared to the specimens already described in Muizon & Cifelli (2000).

In the Systematic Palaeontology section below, concerning the data on the locality we refer to Muizon & Cifelli (2000). For the section "Horizon and Age" we refer to Muizon *et al.* (2015, 2018). When necessary the diagnoses provided by Muizon & Cifelli (2000) is emended. The terminology used here for molar morphology follows Muizon & Cifelli (2000: fig. 1).

The measurements of upper molar areas were taken on photographs of occlusal surfaces in kollpaniins, many euungulates (e.g., artiodactyls, perissodactyls, notoungulates, litopterns) and ungulate-like mammals (e.g., "condylarths"), and also on several "cimolestans" used as potential outgroups. The same was also undertaken for lower molars in kollpaniins. Photographs were taken with the occlusal surface and the lens of the camera oriented parallel to each other with a scale placed parallel to, and at the same height as the occlusal plane. Molar outlines were drawn and areas were calculated with the software ImageJ (Rasband 1997-2018) at the level of the collar for brachydont species and at the occlusal surface for hypsodont species. Only hypsodont species with unvarying (or weakly varying) molar dimensions along their crown height were included. No hypselodont species (ever-growing teeth) were included. We plotted the relative molar proportions of each taxon in a morphospace described

by the ratios of molar areas of M2/M1 and M3/M1, as in previous studies interested on molar proportions (e.g., Kavanagh *et al.* 2007; Polly 2007; Wilson *et al.* 2012; Halliday & Goswami 2013; Carter & Worthington 2016) (note that these studies were interested on lower molars, while this part of our study is mainly focused on upper ones; see below). This corresponds to the 'developmental' morphospace as introduced by Polly (2007) and based on the predictive mathematical model of Kavanagh *et al.* (2007) (Inhibitory Cascade Model or IC model), which initially aimed at predicting the diversity in lower molar proportions among murine rodents. Polly demonstrated that Kavanagh *et al.*'s model was also powerful for a wider array of mammals (see also Wilson *et al.* 2012; Halliday & Goswami 2013; Carter & Worthington 2016).

INSTITUTIONAL ABBREVIATIONS

AMNH	American Museum of Natural History, New York, United States;
DGM	Divisão de Geología e Mineralogía do Departamento Nacional da Produção Mineral , Rio de Janeiro, Brazil;
GI-PST	Institute of Geology, Section of Palaeontology and stratigraphy, Mongolian academy of Sciences, Ulaan Baatar, Mongolia;
IITR/SB/VLR	Vertebrate Palaeontology Laboratory, Department of Earth Sciences, Indian Institute of Technology, Roorkee, India;
HGSP	Howard University/Geological Survey of Pakistan, Islamabad, Pakistan;
MACN	Museo Argentino de Ciencias Naturales "Bernardino Rivadavia", Buenos Aires, Argentina;
MCZ-VP	Harvard University, Museum of Comparative Zoology, vertebrate paleontology, Cambridge, Massachusetts, United States;
MNRJ	Museu Nacional e Universidade Federal do Rio de Janeiro, Rio de Janeiro, Brazil;
MHNC	Museo de Historia Natural "Alcide d'Orbigny", Cochabamba, Bolivia;
MHNM	Natural History Museum of Marrakech, Morocco;
MLP	Museo de La Plata, La Plata, Argentina;
MNHN.F	Muséum national d'Histoire naturelle, Palaeontological collection, Paris, France;
NMMNH	New Mexico Museum of Natural History and Science, Albuquerque, NM, United States;
PSS-MAE	Paleontological and stratigraphy Section (Geological Institute), Mongolian Academy of Sciences, Ulaan Baatar, Mongolia;
RR	Rangarao-Obergfell Trust for Geosciences, Dehra Dun, India;
UALVP	University of Alberta, Department of Biological Sciences, Laboratory for Vertebrate Paleontology, Edmonton, Canada;
UCMP	Museum of Paleontology, University of California, Berkeley, United States;
UM	University of Michigan Museum of Paleontology, Ann Arbor, Michigan, United States;
USNM	United States National Museum, Smithsonian Institution, Washington, DC, United States;
YPFB	Yacimientos Petrolíferos Fiscales de Bolivia;
YPM-PU	Princeton University collection housed in the Yale Peabody Museum, Yale University, New Haven, Connecticut, United States;
Z. Pal	Paleontological Institute of the Polish Academy of Sciences, Warsaw, Poland.

SYSTEMATIC PALEONTOLOGY

Order PANAMERIUNGULATA Muizon & Cifelli, 2000
Family MIOCLAENIDAE Osborn & Earle, 1895
Subfamily KOLLPANIINAE
Marshall, Case & Woodburne, 1990

Molinodus suarezi Muizon & Marshall, 1987

EMENDED DIAGNOSIS. — Size similar to that of *Promioclaenus*; dental formula I?/3, C?/1, P?/4, M3/3; P3 triangular, with a strong parastyle anterior to paracone; pre- and postparacristae well-developed; protocone is a well-developed cusp and distincly individualized from the paracone but slender with slight pre- and postcingula; P4 more massive, shorter, and wider than P3, with small conules; protocone only slightly larger than on P3 but more massive; well-marked pre- and postcingula, and strong labial cingulum; M1 triangular and almost symmetrical in relation to its transverse axis; protocone transversely compressed with an oval-shaped apical wear facet; metacone only slightly lingual to the paracone; well-developed cingula (pre-, post- and labial); styles slightly to not projected labially; no hypocone; M2 subquadrangular and strongly asymmetrical, with oblique labial edge; well-developed pre- and postcingula, not reaching the para- and metastyles (but close to them); labial cingulum very strong; protocone large, bulbous, and mesiodistally elongated with incipient duplication; conules large; well-developed para- and metacingula reaching para- and metastyles; paracone higher and more voluminous than metacone; metacone much more lingual than paracone; centrocrista straight; para- and metastyles almost aligned with para- and metacones but parastyle still slightly shifted labially; no well-individualized hypocone; M3 much wider than long; strongly bent posteriorly; labial edge strongly oblique; little reduced (i.e. only slightly shorter than M2); metacone and metaconule reduced; i1 and i2 distinctly larger than i3; i2 staggered; lower canine short and robust; p1 single-cusped, single-rooted, and procumbent; p2 triangular in lateral view; transversely flattened; small posterior cusp; p4, much larger; variable in shape from triangular to quadrate, with a large metaconid appressed against protoconid; anterior crest of protoconid possessing a tiny paraconid; large talonid cusp; lower molars with bulbous cusps; trigonid and talonid basin reduced; strong pre- and small postcingulids (on m1 and m3 only); paraconid clearly smaller than and appressed against metaconid; paracristid transverse and arched distally; metaconid distolingual to and slightly smaller than protoconid; cristid obliqua variable in size and reaching labial edge of metaconid; talonid basin small and open lingually (more an oblique groove than a basin); hypoconid large, inflated, circular, and only slightly smaller than protoconid; entoconid and hypoconulid almost completely fused forming a distolingual oblique crest; talonid of m3 larger than on m1-2 with hypoconulid as large as hypoconid. On the dentary presence of a well-developed coronoid crest separated from the labial edge of m3 by a coronoid fossa.

Among Tiupampa "condylarths", *Molinodus* more resembles *Simoclaenus* than the other taxa. However, *Molinodus* differs from *Simoclaenus* in its smaller size, its cheek teeth more elongated mesiodistally, its upper molar less transverse, its M2 more asymmetrical with an mesiolabially projected parastyle, its procumbent p1, and its longer rostrum.

Molinodus differs from *Promioclaenus* in its molars, which are more bulbous with apices of the cusps more approximated, in the longer trigonid of the lower molars with a paraconid less appressed against the metaconid, in the presence of a generally distinct labial cingulum, in the non-reduced m3, in the more transverse and less bulbous upper molars, in the thinner postcingulum, in the strong asymmetry of the M2 with an mesiolabially projecting parastyle, and in the unreduced M3.

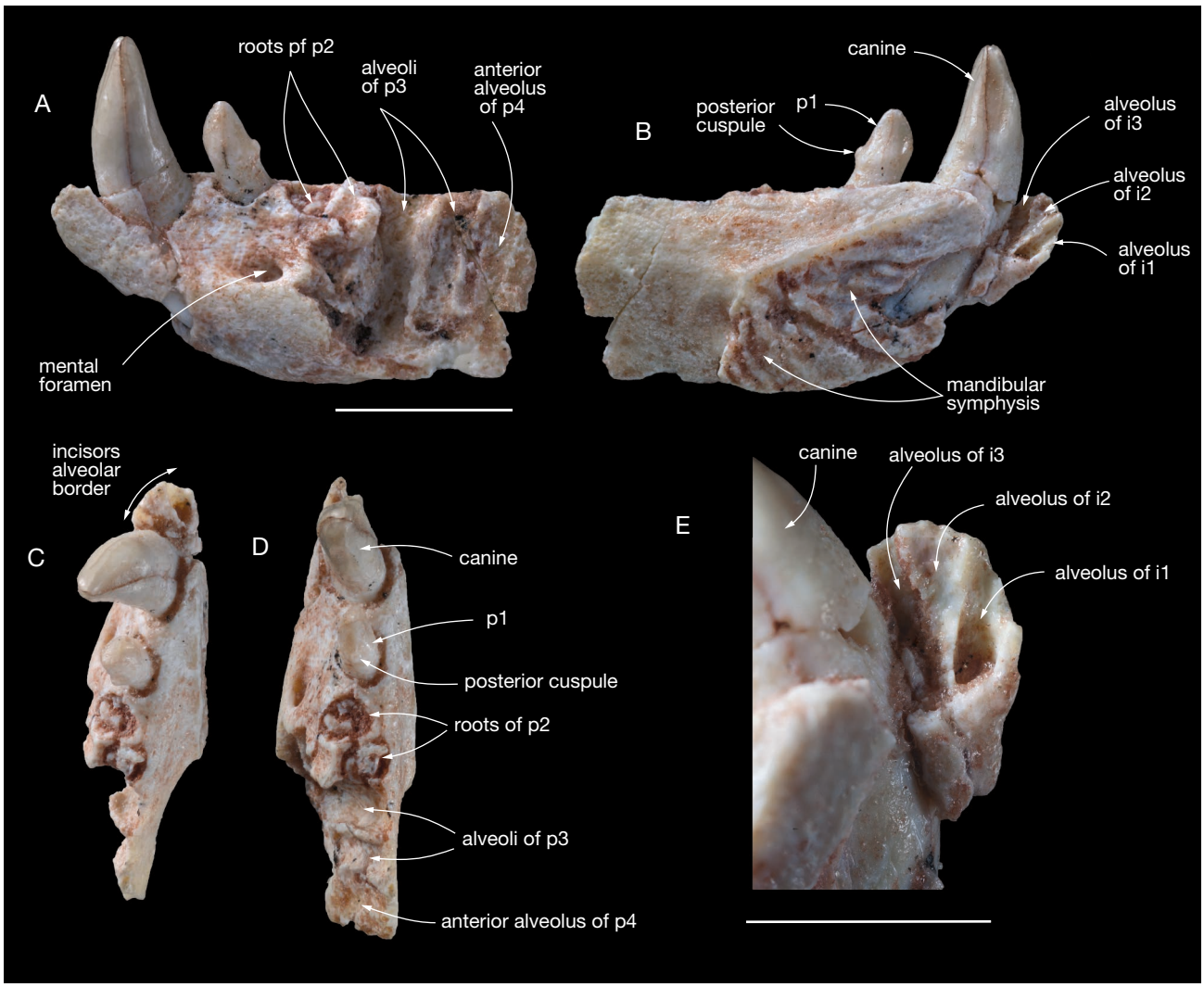

Fig. 1. — *Molinodus suarezi*: anterior portion of a right mandible (MHNC 13883) bearing the alveoli of I1-3, the canine, the p1, the roots of p2, partial alveoli of p3 and the lateral wall of the anterior alveolus of p4 in: **A**, labial view; **B**, lingual view; **C**, anterodorsal view; **D**, dorsal view; **E**, medial view of the lateral wall of the incisors showing the V-shaped morphology of the alveolus of i2, which indicates that the tooth was staggered. Scale bar A-D: 5 mm; E, 3 mm.

Hypodigm. — As in Muizon & Cifelli (2000) with the additional following specimens: MHNC 13883, a partial left mandible with alveoli of incisors, canine, p1, roots of p2, alveoli of p3 and alveolus of anterior root of p4; MHNC 13867, a partial left mandible with p3-m3; MHNC 13870, a partial left maxilla with M1-M3, with M1 and M2 missing the labial edges of para- and metacones.

Description

An anterior fragment of left mandible of *Molinodus suarezi* (Fig. 1) bears the labial edge of the alveoli of the three incisors, the canine, the p1, the roots of p2, the alveoli of p3, and the anterior alveolus of p4 (MHNC 13883). On the medial aspect of the dentary a large symphyseal surface for the intermandibular suture is present. This surface is in one plane with sharp edges, but it is rough and bears numerous ridges and grooves probably interlocking with the symmetrical surface on the other mandible. The two symphyseal surfaces were therefore tightly attached one to the other, but the symphysis was clearly unfused on this specimen. Although ligamentous, it is likely that the symphysis was quite rigid and allowed little intermandibular movements. Because the roots of p3 extends as far as the ventral region of the dentary leaving no space of a potential unerupted tooth germ, we regard that the definitive p3 was erupted. Because the preserved teeth (c and i1) are absolutely unworn, this specimen is interpreted as belonging to a young adult. It is, therefore, not impossible that ontogenetically older individuals may have had a fused symphysis.

On the labial side of the dentary a large anterior mental foramen is present ventral to the embrasure between p1 and p2.

Although the incisors are missing, the anteriormost region of the dentary is preserved with the labial edge of the incisors alveoli. The dentary is broken vertically in this region and the lingual portion of the alveoli is missing; therefore, a vertical section of the incisors alveoli can be observed. Based on the size of the roots, i1 was apparently the largest of the three incisors or was, at best, similar in size to i2. The i3 is clearly the smallest of the three incisors. Interestingly, the alveolus of i2 presents a distinct lingual shift of its root. As a consequence, the vertical section the alveolus is clearly triangular whereas

Fig. 2. — Partial left mandible of *Molinodus suarezi* (MHNC 13867) bearing p3-m3: **A**, stereophotographs of the occlusal view; **B**, lingual view; **C**, labial view. Scale bar: 5 mm.

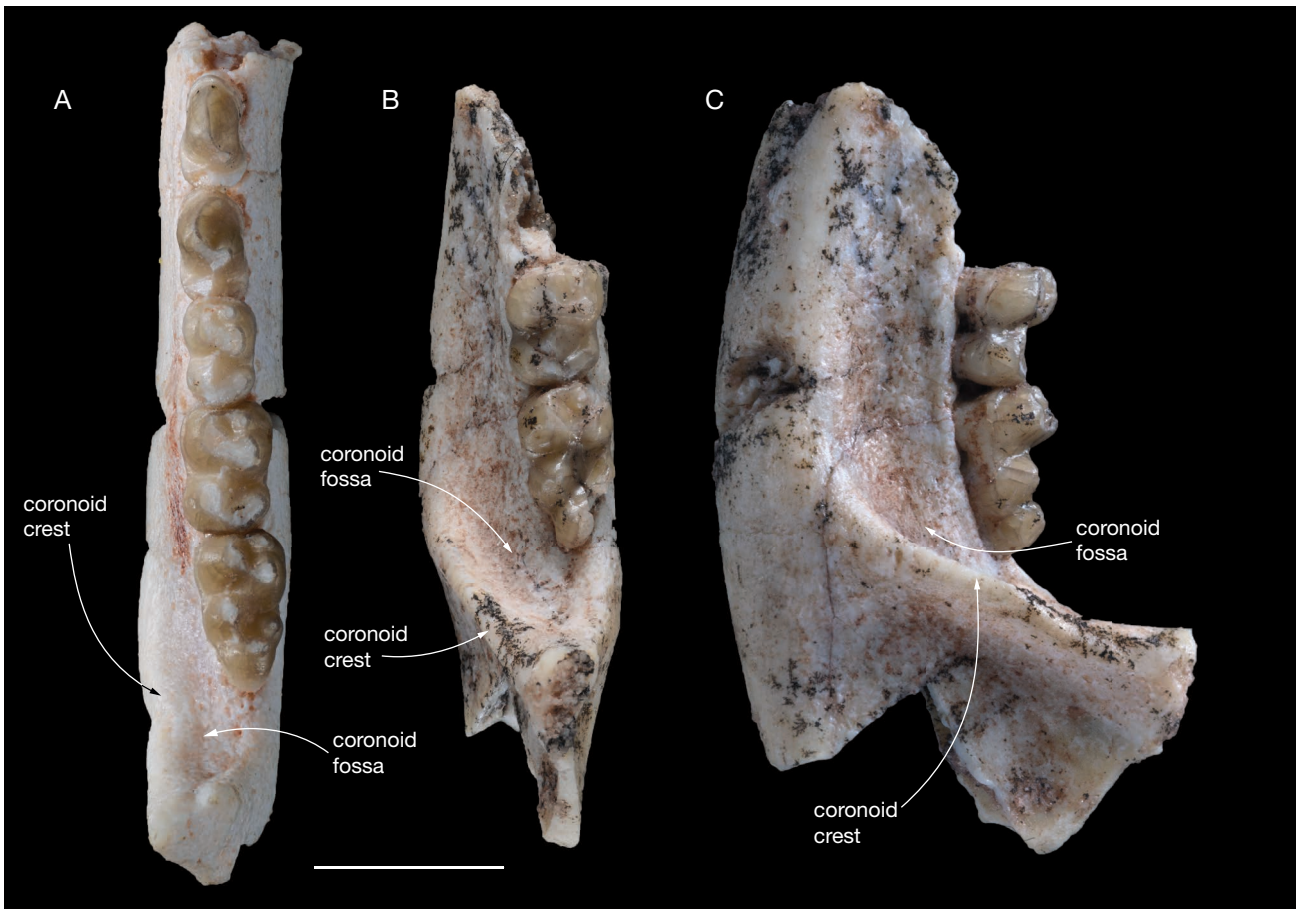

FIG. 3. — *Molinodus suarezi*: **A**, dorsal view of MHNC 13867; **B**, dorsal view of a partial left mandible bearing m2-3 (MHNC 13871) showing the robust extension of the coronoid crest on the lateral side of the dentary and the deep fossa, which separates the crest from the talonid of m3; **C**, the same in labial view. Scale bar: 5 mm.

that of the other alveoli are cylindrical with parallel edges (Fig. 1B, E). This condition of the i2 of *Molinodus*, is identical to the staggered second incisor, (the i3 according to Hershkovitz 1982, 1995), of many metatherians (e.g., stagodontids, pucadelphyids, sparassodonts, didelphids, microbiotheres, peramelids, thylacinids, dasyurids). The triangular section of the alveolus of the staggered incisor is clearly observed on the figure 5 of Hershkovitz (1982). It is not the first time that a staggered second incisor is described in a eutherian since Hershkovitz (1982: 197) mentions this condition in several extant Carnivora. Among the Tiupampa eutherians, it is absent in *Alcidedorbignya inopinata* (Muizon *et al.* 2015), and there is no indication that it was present in *Tiuclaenus minutus* and *Pucanodus gagneri*, the only other Tiupampa eutherians that preserve the anterior portion of the dentary. It may be the first time that this trait is observed in a fossil eutherian, but this is probably due to the fact that the anterior portion of the dentary is rarely preserved in fossil mammals.

In dorsal view, the three lower incisors are set in a slightly oblique row, relative to the symphyseal plane (Fig. 1C). In other words, i1 is anteromedial to i2, and i3 is posterolateral to i2. The lower incisor tooth row was, therefore, more or less parabolic or V-shaped. The last incisor, i3, was closely appressed against the mesial edge of the canine as indicated by the position of the i3 alveolus. The canine is a moderately developed tooth but it is robust. The height of the crown (4.60 mm) is approximately twice its mesio-distal length (2.44 mm) at base.

The canine is transversely compressed, being distinctly narrower (1.75 mm) at its base than long (2.44 mm). The posterior curvature of the canine is weak and its posterior edge is only very slightly concave. Its mesial edge is distinctly convex. On the mesiolingual edge of the tooth a blunt ridge extends mesioventrally on the dorsal half of the crown and distoventrally on the ventral half (Fig. 1B). In dorsal view, the labial side of the canine is strongly convex, whereas it is almost flat to slightly concave on its lingual side. In labial view the main axis of the crown is moderately oblique in relation to the alveolar plane, with which it forms an angle of approximately 110°.

TABLE 1. — Comparative measurements (in mm) of the lower molar in *Molinodus suarezi*. Abbreviations: **L**, length; **W**, width of trigonid.

	m1 L	m1 W	m2 L	m2 W	m3 L	m3 W
YPFB Pal 6112	3.15	2.34	3.69	2.82	3.98	2.43
YPFB Pal 6113	3.47	2.89	3.78	3.30	4.30	–
MHNC 8269	3.13	2.30	3.60	2.74	4.72	2.80
MHNC 13867	3.29	2.20	3.83	2.71	4.71	2.71

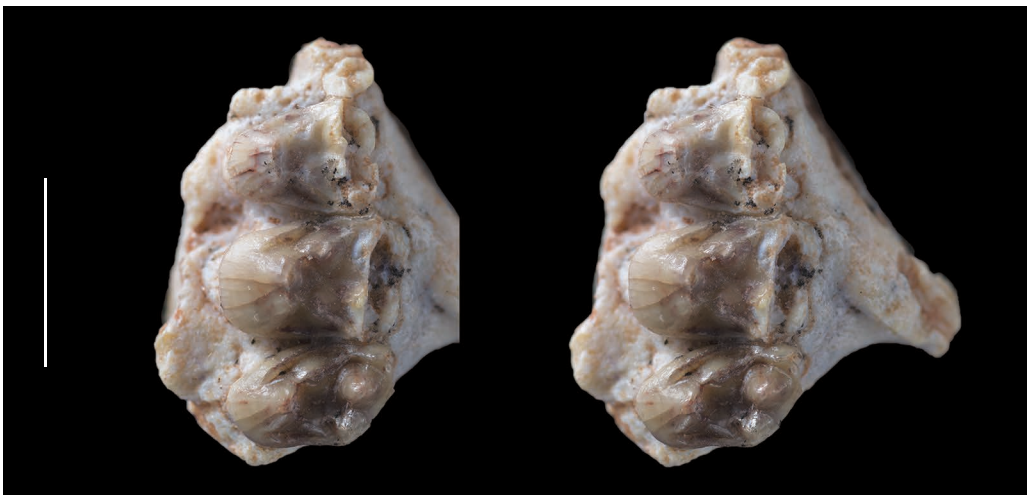

Fig. 4. — *Molinodus suarezi*: partial maxilla (MHNC 13870) with incomplete M1-2 and complete M3. Stereophotograph of occusal view. Scale bar: 5 mm.

Posterior to the canine is a small p1 separated from the former by a small but distinct diastema. The p1 is single-rooted. It is slightly procumbent and asymmetrical in labial view. The crown of the tooth is markedly compressed transversely. It bears a pronounced mesial crest, which is slightly convex. The distal edge of the tooth is straight and bears a small cuspule at its base (Fig. 1D). There is no cingulum at the base of the crown. The lingual aspect of the crown in markedly concave and its labial edge is convex. As a consequence, in distal view the crown is slightly bent lingually.

The roots of p2 are preserved in the dentary of MHNC 13883. The very short diastema, which separates p2 from p1, is approximately twice shorter than the diastema anterior to p1. A similar condition is observed on MHNC 1243, a mandible fragment, which preserves the root of c, the alveolus of p1 and p2 (see Muizon & Cifelli 2000). Interestingly, on MHNC 13883 the roots of p2 are set obliquely in the dentary and the anterior root is mesiolabial to the posterior one. The mesiodistal axis of the tooth is approximately at an angle of 30° with the anteroposterior axis of the tooth row (from c to p4) (Fig. 1D). Because this condition is not present in MHNC 1243, it could represent a pathological condition or an individual variation in MHNC 13883. Posterior to p2, the alveoli of p3 indicate that the tooth was implanted parallel to the axis of the tooth row. The p2 and p3 were not separated by a diastema and were closely appressed one against the other.

A relatively complete left mandible of *Molinodus suarezi* (MHNC 13867) bears p3-4 and m1-3 (Fig. 2). The most interesting element of this specimen lies in its premolars. The teeth are relatively narrow transversely being *c.* 30% longer than wide. They are roughly triangular in lateral view and are approximately as high as long. The p3 is slightly more slender than the p4 but both teeth are built on a similar pattern. The mesial edge of p3 bears a sharp crest with a marked angulation on the dorsal third of the crown. The largest cusp of the tooth, the protoconid, is transversely narrow and its lingual edge is slightly concave lingually, in its dorsal region. More ventrally it is inflated and convex. The distolingual angle of the protoconid bears a strong inflation, which reaches the dorsal half of the distal edge of the tooth in lingual view. This structure corresponds to the development of a small metaconid. At the mesial base of the tooth is a small cingulum, which is continuous from the distolabial to distolingual edges of the mesial root. Distally a well-developed talonid cusp forms the base of the crown and extends transversely in a robust and rounded cingulum from the distolabial to the distolingual angle of the tooth. In occlusal view, p3 is distinctly wider distally than mesially.

The p4 is slightly longer than the p3. Its mesial edge bears a sharp crest that shifts lingually at mid-height of the crown. There, it forms a small tubercle interpreted as an incipient paraconid. The protoconid is strongly convex labially and flat lingually. On its distolingual edge is a large metaconid. In dorsal view, it is slightly smaller than the protoconid and its apex is distinctly distal to that of the protoconid. On the mesial edge of the protoconid, a sharp and well-developed paracristid connects to the paraconid mesially. Posterior to the trigonid, the talonid does not bear differentiated cusps but forms a thick distobasal ridge, which extends from the mesiolingual to mesiolabial aspects of the distal root. The distal edge of the tooth is slightly wider than the mesial one.

The condition of the p4 of MHNC 13867 distinctly departs from the morphology of the isolated p4 (MHNC 1244) referred to *Molinodus suarezi* by Muizon & Cifelli (2000: fig. 3M, N). On MHNC 1244 the metaconid is almost totally lingual to the protoconid and not shifted distally. Furthermore, the crown of the tooth is markedly more massive, strongly compressed mesiodistally, and more inflated transversely. As a whole, MHNC 1244 more resembles the p4 of *Simoclaenus sylvaticus* in all its features but is clearly much smaller. When compared to the size of the roots observed on the holotype of *S. sylvaticus*, it is even too small to be a p3 of and it is also slightly too small to be a p2. In other respects, the large metaconid and the well-developed paraconid and paracristid of MHNC 1244 are more compatible with the morphology generally observed on a p4. Therefore, we think that MHNC 1244 is actually a

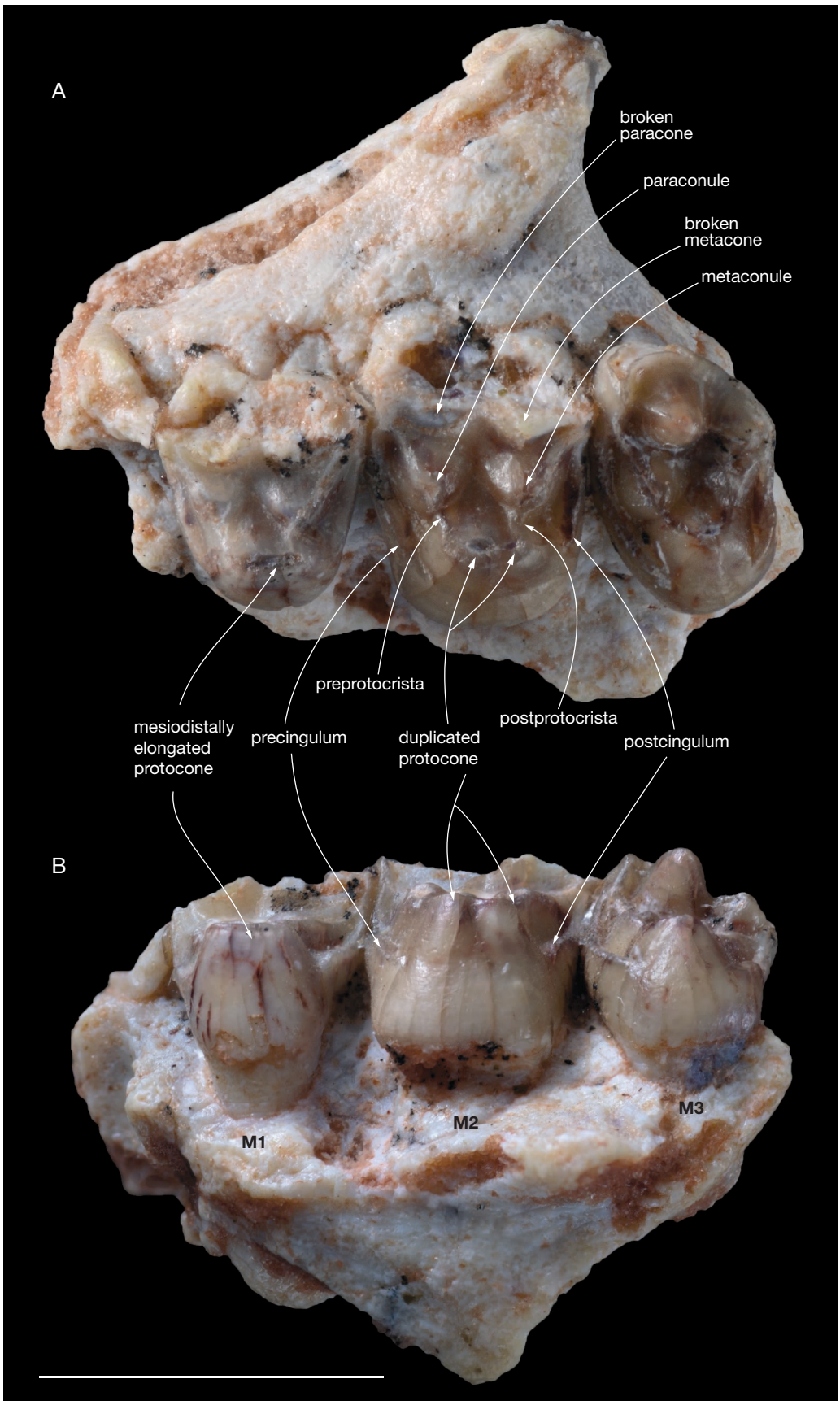

Fig. 5. — *Molinodus suarezi*: partial maxilla (MHNC 13870): **A**, occlusal view; **B**, lingual view. Scale bar: 5 mm.

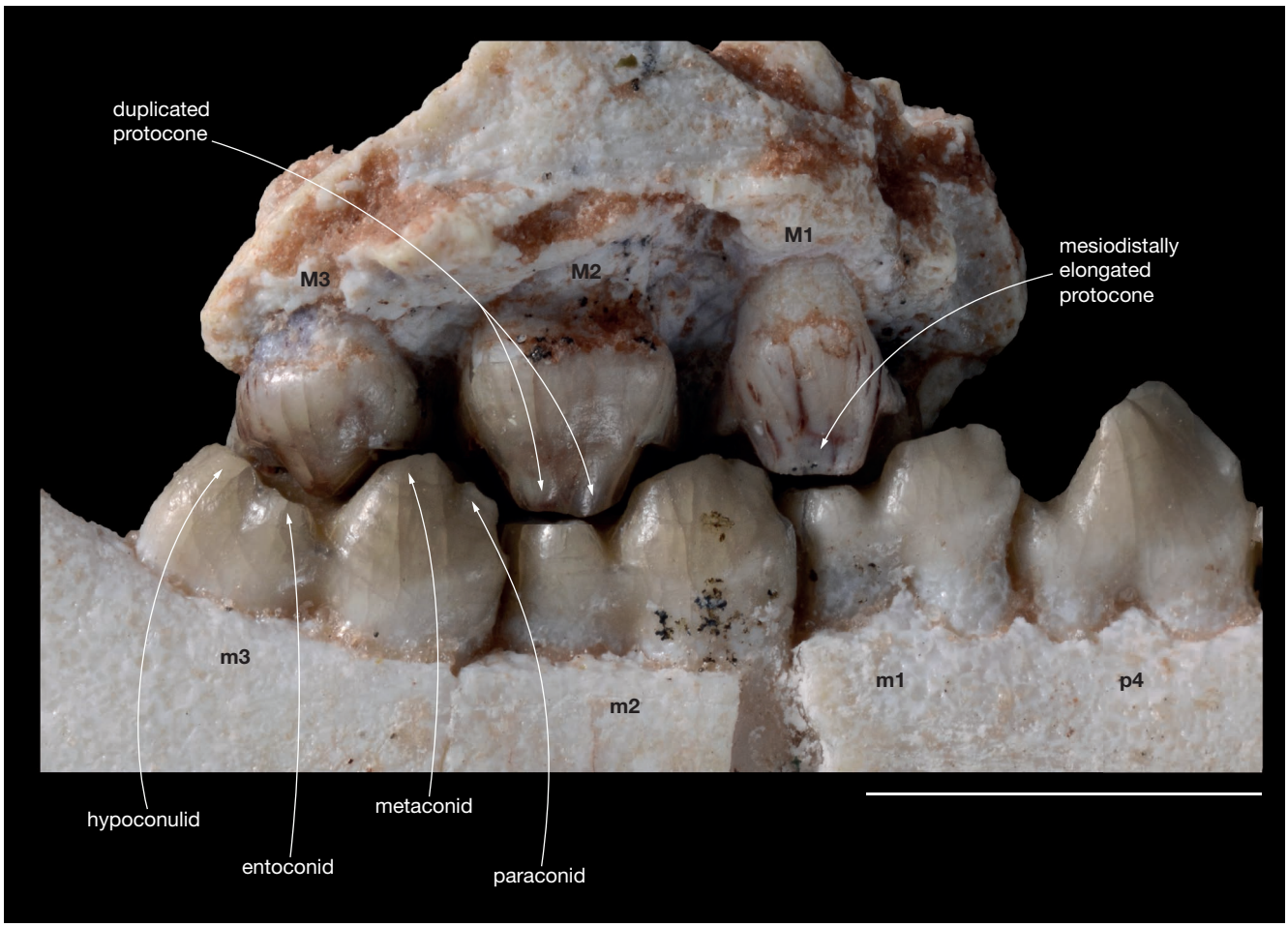

Fig. 6. — *Molinodus suarezi*: composite occlusion of the maxilla MHNC 13870 and the mandible MHNC 13867 in lingual view. Scale bar: 5 mm.

p4 and that, either, the morphology of the p4 of *M. suarezi* is highly variable or MNHC 1244 represents a new taxon at Tiupampa. Given the size difference it is unlikely that it could be referred to *S. sylvaticus*, except if this species is sexually dimorphic, which is unknown yet. However, given the lack of a representative sample of *M. suarezi* and *S. sylvaticus*, this uncertainty cannot be resolved so far.

The three molars have the characteristic features of *Molinodus suarezi* as described by Muizon & Cifelli (2000). The trigonid bears a well-developed paraconid but distinctly smaller than the metaconid and placed mesial to it or slightly labial (on m1). The paraconid is closely appressed against the metaconid. The latter is large, almost as large as the protoconid and located distolingual to it. As a consequence, the protocristid is obliquely oriented (mesiolabially-distolingually) as compared to the axis of the tooth row. On m1 and m2 the talonid is slightly narrower than the trigonid. The cristid obliqua extends from the large hypoconid to the central region of the protocristid. Lingually, the hypoconulid and the entoconid are connate and the talonid basin is in fact an obliquely oriented groove that opens mesiolingually as is observed in all kollpaniines. On m3 the hypoconulid is much larger than on the other molars and is as large as the hypoconid.

The small size of the m1 relatively to the other molars is noteworthy. This feature is present in all kollpaniines but it is especially pronounced in the holotype (YPFB Pal 6112) of *M. suarezi* (Muizon & Cifelli 2000: fig. 3A) and MHNC 13867 (Table 1).

On the dentary of MHNC 13867, the posteriormost mental foramen is located below the anterior root of p4. The corpus mandibularis of MHNC 13867 and 13871 is relatively massive especially in the latter. On both specimens, most of the ramus mandibularis is missing, except the anterior portion of the coronoid process. In the region of the retromolar space, the anterior basis of the coronoid process is very wide and bears a conspicuous labially opening coronoid fossa. The fossa is much deeper on MHNC 13871 than on 13867. Lateral to the fossa, the coronoid crest is salient and extends ventrally on the lateral aspect of the dentary (Fig. 3). This condition indicates a powerful masseter muscle, which inserts in the masseteric fossa and on the coronoid crest and is congruent with the stoutness of the corpus mandibularis. A robust coronoid crest is observed on the other specimens of *M. suarezi* (YPFB Pal 6114, MHNC 8269) and on the large kollpaniines (*Simoclaenus* and *Andinodus*). It is absent or barely present in *Tiuclaenus* and *Pucanodus*, which are the smallest kollpaniine taxa (see Muizon & Cifelli 2000).

A partial left maxilla referred to *Molinodus suarezi* (MHNC 13870) bears the three molars and is the first specimen discovered with an M3 associated to the anterior molars (Figs 4; 5; 6). The M3 referred by Muizon & Cifelli (2000: fig. 2, E) to *M. suarezi* is an isolated specimen and its referral had yet to be confirmed. M1 and M2 of MHNC 13870 are incomplete and are missing most of the labial edges of the para- and metacones and all the stylar regions and labial cingulum. M3 of MHNC 13870 is complete.

M1 and M2 of MHNC 13870 preserve the lingual half of the tooth. The large protocone bears large conules which are similar to those already described in *Molinodus*. The mesial and distal edges of M1-2 present well-developed pre- and postcingulae, which extended labially until the stylar area of the teeth. The most interesting cusp of this specimen is the protocone. On M1-2 as is observed on the molars of *M. suarezi* described by Muizon & Cifelli (2000), the protocone is mesiodistally elongated and its wear facet is markedly ovale-shaped. On the M2 of MHNC 13870, the wear facet is constricted and the protocone bears vertical grooves, which reach the apex of the cusp. As a consequence, the latter is distinctly bilobate (Fig. 5). The posterior lobe of the protocone of MHNC 13870 receives the postprotocrista, which links it to the metaconule. This bilobate condition is even more pronounced than in MHNC 8280 (Muizon & Cifelli 2000: fig. 2A) as it concerns more than the apex of the cusp and extends dorsally on the protocone. It indicates that the duplication of the apical region of the protocone was almost certainly observable on the dentine at the enamel-dentine joint (see Anemone *et al.* 2012).

The M3 of MHNC 13870 is remarkably similar to the isolated tooth referred to *Molinodus suarezi* by Muizon & Cifelli (2000) and does not require further description.

Simoclaenus sylvaticus Muizon & Cifelli, 2000

EMENDED DIAGNOSIS. — Dental formula: I ?/?, C 1/1, P 4/4, M 3/3; relatively large short-snouted kollpaniine characterized by the strong mesiodistal compression of its lower molars and premolars, which is correlatively observed on the M2; upper canine transversely compressed; P1 vertically implanted; P2 with a small protoconal bulge on lingual side of paracone; P3-4 with well-developed protocone (slightly larger on P4); M1 much smaller than M2; M2 almost square in occlusal outline but distinctly asymmetrical as in *Molinodus*; p4 with a well-developed metaconid medial to protoconid; molars with a large metaconid, posterior to the protoconid and with a posterior projection that partially fills the talonid basin; protoconid distinctly smaller than in *Andinodus*; posterior wall of trigonid sigmoid in occlusal view; paraconid and paracristid smaller than in *Andinodus*; large hypoconid with a labial slope less vertical than in *Andinodus*; cristid obliqua meets trigonid on lingual edge of protoconid.
Ascending process of the maxilla short, high, and erected, premaxilla-maxilla suture subvertical in lateral view; frontal-maxilla suture present (therefore absence of nasal-lacrimal suture) anterior opening of infraorbital canal at level of P3. Rostrum, blunt and short as indicated by cheek teeth mesiodistal compression, implantation of anterior premolars, and subvertical premaxilla-maxilla suture.

HYPODIGM. — The type specimen, MHNC 8332, a fairly complete right dentary with the alveoli of c, p1, the roots of p2, the alveolus of p3, and p4-m3. The dentary is lacking the anterior region with the incisor alveoli and most of the coronoid process; MHNC 8348, a right maxilla with M1 lacking the parastylar region and part of the paracone and M2-3 complete; MHNC 13868, a right maxilla with root of the canine and P1-P4; MNHC 13872, a partial mandible with alveolus of p1, roots of p2-3and p4-m1; MHNC 13876 a right maxilla fragment with M1-M2.

TABLE 2. — Proportions of p4 and m1 in the holotype and in the new specimen of *Simoclaenus sylvaticus* (in mm).

	MHNC 8348 (holotype)	MHNC 13872	ratio
Length of p4	3.46	2.97	14%
Width of p4	3.20	2.84	10%
Length of m1	3.71	3.58	3%
Width of trigonid of m1	3.48	3.04	13%

TABLE 3. — Proportions (in mm) at alveolar border of the upper canine of *S. sylvaticus* as compared to the lower canine of *M. suarezi*.

	MHNC 13883 *Molinodus suarezi* (lower canine)	MHNC 13868 *Simoclaenus sylvaticus* (upper canine)	ratio
Length of canine at alveolar plane	2.44	4.58	87%
Width of canine at alveolar plane	1.75	2.72	55%

TABLE 4. — Proportions (in mm) of the P3 and P4 of *S. sylvaticus* and *M. suarezi*.

	P3		P4	
	S. sylvaticus (MHNC 13868)	*M. suarezi* (MHNC 1247)	*S. sylvaticus* (MHNC 13868)	*M. suarezi* (MHNC 1247)
Length	3.35	3.02	3.17	2.74
Width	3.56	3.46	3.98	3.82

DESCRIPTION

Three new specimens are referred to this species. MHNC 13872 is a mandible fragment with the alveolus of p1, the roots of p2-3 and p4-m1 (Fig. 7). The alveolus of p1 is vertical as in the holotype of *Simoclaenus sylvaticus* (MHNC 8332) (Muizon & Cifelli 2000), indicating that the tooth was not procumbent in contrast to the condition observed in *Molinodus* (see above). This feature, shared by the holotype of *Simoclaenus sylvaticus* and the new specimen clearly supports the referral of the latter rather than to *Molinodus suarezi*, the p1 of which is procumbent (Fig. 1A, B). However, the major characteristic of this specimen lies in its p4, which is markedly compressed mesiodistally as is observed on the holotype. As in the latter, the metaconid is placed lingually to the protoconid and is not shifted posteriorly as is observed in *Molinodus suarezi* (Fig. 1D). Furthermore, the p4 of MHNC 13872 has the same strongly bulbous morphology as that of the holotype. The m1 is relatively worn but does not depart significantly from that of the holotype in terms of morphology.

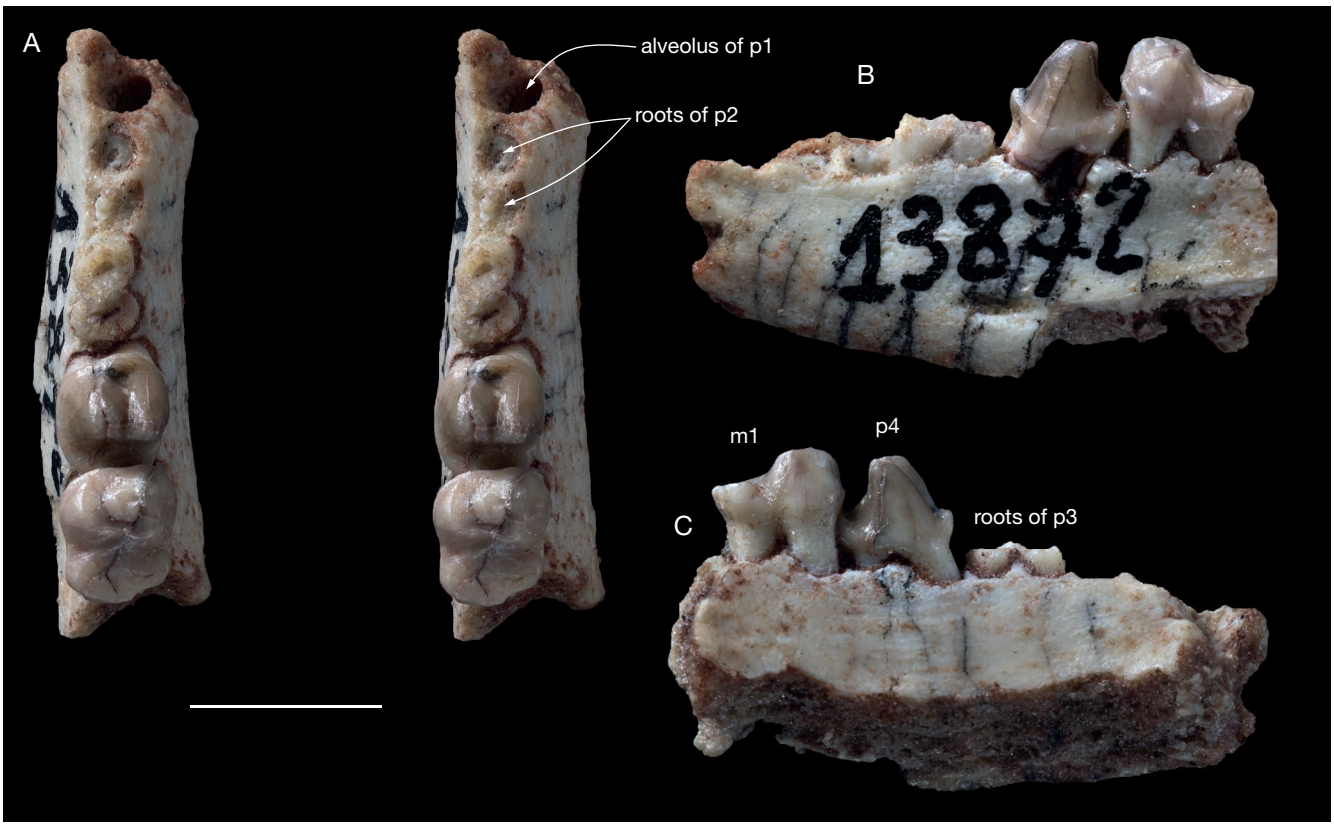

FIG. 7. — *Simoclaenus sylvaticus*: partial right mandible with alveolus of p1, root of p2-3, p4 and m1 (MHNC 13872): **A**, stereophotographs of occlusal view; **B**, the same in lateral view; **C**, the same in medial view. Scale bar: 5 mm.

However, the two specimens differ in their size and the new specimen described here is distinctly smaller than the holotype (Table 2). As a matter of fact, the p4 and m1 of the new specimen are in average 10% smaller than those of the holotype (mean of the four ratios of Table 2). Although significant, this difference could be interpreted as related to individual size variation. The other large "condylarth" to which this specimen could be related is *Molinodus suarezi*, although this taxon is clearly smaller than *Simoclaenus sylvaticus*. However, the p4 observed on the mandible of *M. suarezi* described above (Fig. 2A) is so different from that of MHNC 13872 that we rather favor a strong individual size variation in *S. sylvaticus* than morphological variation in *M. suarezi*.

A well-preserved lateral ascending process of a right maxilla (MHNC 13868) is referred to *Simoclaenus sylvaticus*. This specimen bears the root of the canine and the four premolars, which were unknown for this taxon (Fig. 8). The upper premolars of MHNC 13868 are only slightly larger than those of *Molinodus suarezi* described by Muizon & Cifelli (2000: 59), but this difference could be interpreted as related to individual variation in size. The major criterion that convinced us to relate this specimen to *S. sylvaticus* is the size of the canine. Although the crown of that tooth is not preserved the section of the root at the level of the alveolar border is relevant to its size. It is noteworthy that no upper canine is known for *M. suarezi*. We therefore compared the section of the upper canine of MHNC 13868 to that of the lower canine of MHNC 13883. Because the Tiupampa kollpaniines are relatively unspecialized, it is hypothesized that the width and length (at the level of the alveolar plane) of the upper and lower canines did not differ significantly even if generally the upper canines are slightly larger than the lowers. This remains an assumption, as no kollpaniine has ever been documented by both upper and lower canines.

Here, the upper canine of MHNC 13868 (*Simoclaenus*) is 87% longer and 55% wider than the lower canine of MHNC 13883 (*Molinodus*) (Table 3). Even taking into account the approximation in comparing upper and lower canines, such a size difference is highly significant and we regard as unlikely that the two canines could belong to the same taxon of kollpaniine. We therefore, tentatively refer MHNC 13868 to *S. sylvaticus* rather than to *M. suarezi*. Furthermore, the size difference between the P4 and M1 of the holotype of *S. sylvaticus* and referred specimen described here could be related to sexual dimorphism in this species as evoked above.

The premolars are well preserved and bear very reduced dental wear. The size of P3 and P4 is slightly larger than the equivalent teeth in *Molinodus suarezi*, which are known on one specimen only (MHNC 1247) (see Muizon & Cifelli 2000: 58) (Table 4). P1 and P2 are unknown for *M. suarezi*. Although this size difference is moderate (*c.* 10%), because of the large size of the canine, we rather refer this specimen to *Simoclaenus sylvaticus*. Furthermore, the anteroposterior length of the upper premolar row of MHNC 13868 (11.31

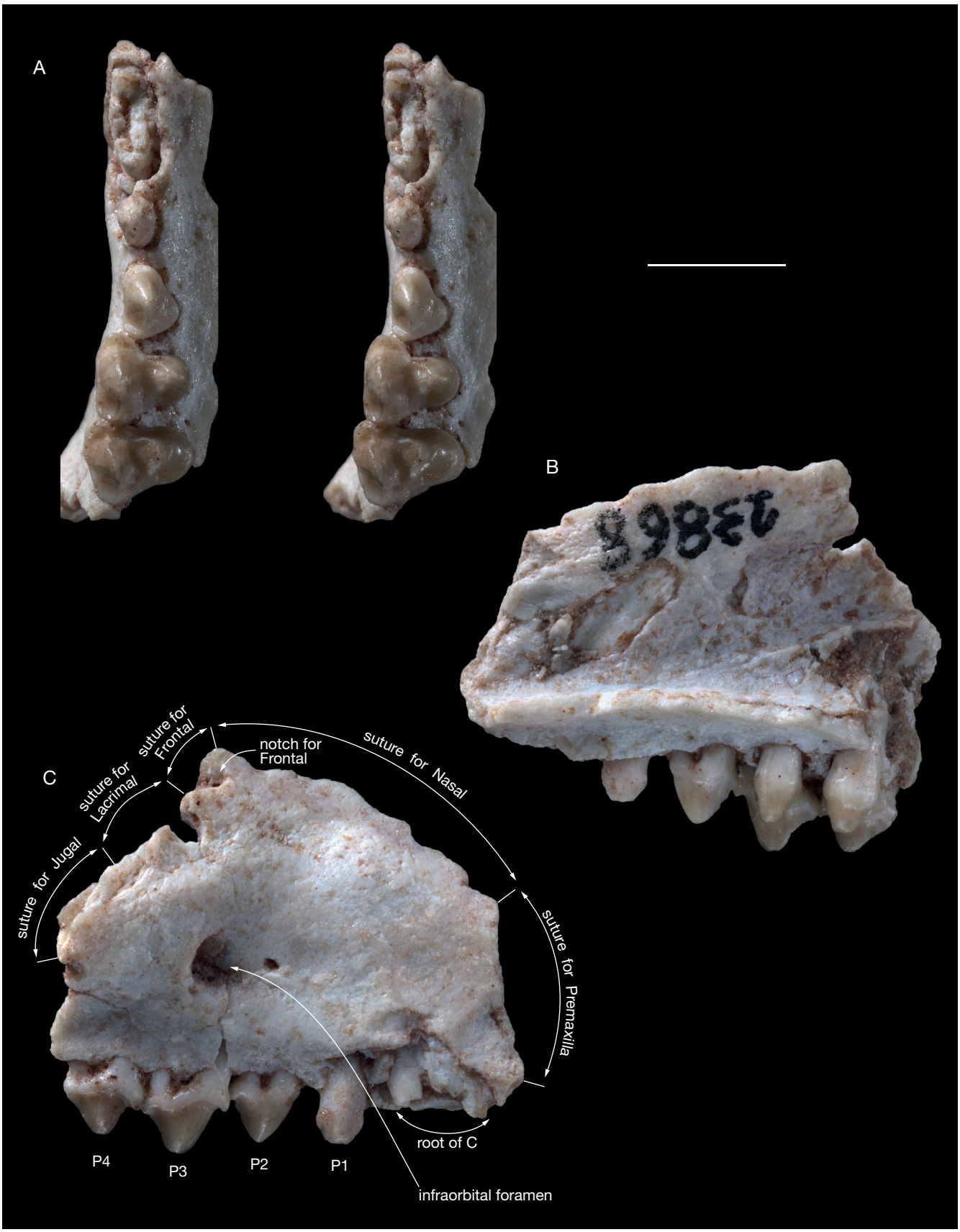

FIG. 8. — *Simoclaenus sylvaticus*: partial right maxilla with root of the canine and P1-4. (MHNC 13868): **A**, stereophotograph of occlusal view; **B**, the same in medial view; **C**, the same in lateral view, with tentative interpretations of bony sutures (see text). Scale bar: 5 mm.

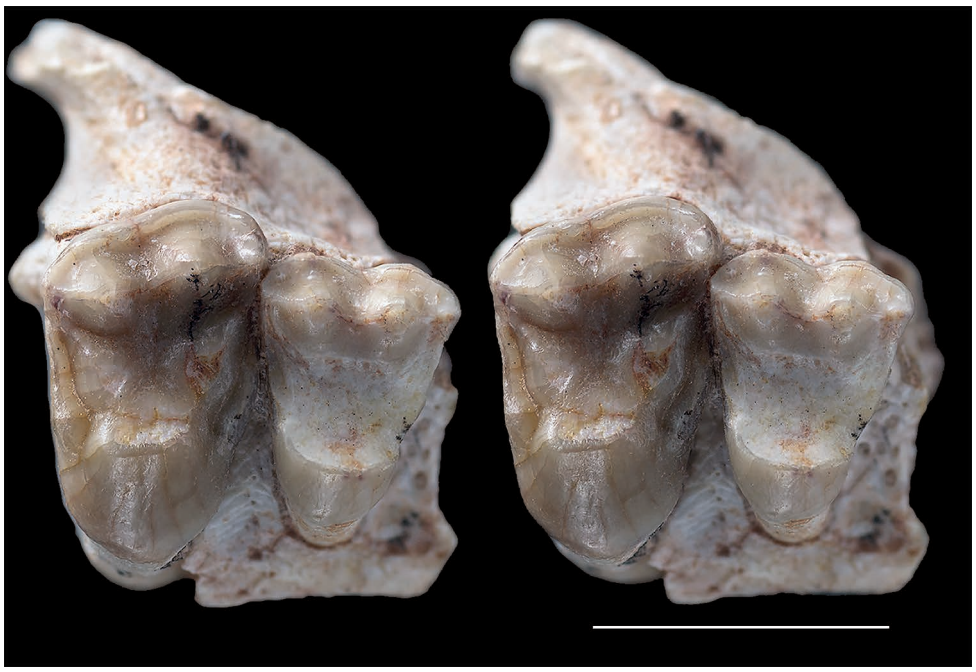

FIG. 9. — *Simoclaenus sylvaticus*: partial right maxilla with M1-2 (MHNC 13876), stereophotograph of occlusal view. Scale bar: 5 mm.

mm) is only slightly smaller than the lower premolar row of the holotype of *S. sylvaticus* (11.97 mm), on which the alveoli of p1-3 and the p4 are preserved. Therefore, the mesiodistal length of the upper premolar row of the new specimen (MHNC 13868) correctly matches the length of the lower premolars row of the holotype (MHNC 8348).

P1 is peg-like, single-rooted, and compressed transversely. It is implanted vertically in the maxilla as is observed on the alveolus of the p1 of the holotype (MHNC 8348). This condition suggests a relative shortness of the rostrum and is congruent with the anteroposterior compression of the lower cheek teeth observed on the mandible. It is noteworthy that the p1 of *Molinodus* described above (MHNC 13883) differs from the condition observed in *Simoclaenus* in being slightly procumbent, thus suggesting a more elongated rostrum. As preserved, the P1 of *Simoclaenus* on MHNC 13868 is longer than high and no significant wear facet can be observed at the apex of its crown. In lateral view the tooth is roughly symmetrical anteroposteriorly. A small diastema separates P1 from the canine anteriorly and from P2 posteriorly. P2 is triangular in occlusal view and bears three roots. It is longer than wide. It presents a conspicuous inflation on its distolingual edge, which can be regarded as an incipiently developed protocone (protoconal bulge). The paracone forms most of the tooth and is as high as long. Its mesial edge is wide and blunt whereas its distal edge is thin and forms a sharp crest. The tooth bears no cingulum but a small cusp at the distolabial edge of the paracone could be regarded as a metastyle. This style contacts the anterior edge of P3 and no diastema separates the two teeth. P3 is slightly wider than long, triangular in occlusal view, and bears three roots. The mesial and distal edges are markedly concave, a condition which individualizes a well-developed protocone lingually. This cusp is approximately two thirds the height of the paracone. It is as long as wide. It has a very convex lingual edge and a flat labial aspect. These two edges of the tooth are separated by sharp pre- and postprotocristae, which join the base of the crown at the level of the greatest concavity of the mesial and distal edges of the tooth. Labially the paracone is approximately twice as long as wide. Its mesial edge bears a smooth crest and its distal crest is slightly obliterated by an elongated wear facet, which extends from the apex of the tooth to the posterior base of the paracone. At the mesial angle of the paracone is a marked parastyle. From this cusp, a conspicuous cingulum extends on labial edge of the paracone. At the distal end of the cingulum is a small metastyle. P4 has a pattern similar to that of P3 but it is mesiodistally shorter and transversely wider. Its mesial and distal edges are slightly concave but to a much lesser extent than the condition observed on P3. The paracone is smaller (in height and volume) and the protocone is more voluminous than on the preceding tooth. The pre- and postprotocristae are more developed than on P3 and extend on the anterior and posterior edges of the paracone. The postprotocrista even joins the distolabial angle of the tooth and contacts the postparacrista. The latter bears a narrow wear facet on its mesial two thirds only. The distal end of the postparacrista bears, on its lingual aspect, a hint of inflation, which can be interpreted as an incipient metacone. A tiny inflation on the postprotocrista may also be regarded as an incipient metaconule. On the distal edge of the protocone, is a distinct postcingulum. On its mesial edge the precingulum is weakly developed. On the mesiolabial angle of the tooth the parastyle is more developed than on P3. From this style, a well-developed labial cingulum extends distally until the metastylar angle of P4.

Little is preserved of the palatal process of the maxilla, but the lateral wall of the rostrum from the anterior edge of the canine to the anterior root of the zygomatic arch is relatively complete and all its edges likely correspond to sutures with adjacent bones except for a small U-shaped-break in the posterodorsal angle (Fig. 8C). The anterodorsal edge of the specimen probably corresponds to the nasal-maxilla suture. Approximately above the P1-P2 embrasure, the edge of the maxilla distinctly protrudes medially. Anterior to this indentation, the suture is apparently anteroposteriorly oriented or slightly oriented anterolaterally. Posterior to it, the suture diverges posterolaterally, thus indicating a widening of the nasals posteriorly, as generally observed in early diverging metatherians and eutherians (e.g., deltatheroidans, pucadelphydans, *Zalambdalestes*, *Kulbeckia*, *Alcidedorbignya*). On the posterior limit of the maxilla, as preserved, is a deep groove probably for the articulation of the anterior process of the jugal. This groove (maxilla-jugal suture) approximately corresponds to the level of the anterior edge of the orbit and the posterior limit of the rostrum, which corresponds to the posterior edge of P4. On the posterodorsal angle of the specimen, in lateral view, is a distinct small notch (dorsal to the breakage notch mentioned above), which was receiving the anterolateral angle of the frontal. If this interpretation is correct, the nasal and lacrimal of *Simoclaenus* were distinctly separated, which likely represents a crown Placentalia condition (frontal-maxilla suture present) (Muizon *et al.* 2015). The posterior edge of the maxilla, between this notch and the dorsal end of the jugal groove, likely corresponds to the lacrimal-maxilla suture. Anteriorly, several grooves mark the edge of the maxilla immediately anterior to the canine, which we interpret as the premaxilla-maxilla suture. This suture is almost straight, slightly concave anteriorly, and sub-vertical, forming an angle of approximately 95° with the alveolar plane (Fig. 8C).

The lateral aspect of the maxilla is markedly elevated and erected, to a greater extent than the condition observed in the pantodont *Alcidedorbignya inopinata* from the same locality (Muizon *et al.* 2015). This condition apparently resembles that of *Baioconodon nordicum* (YPM-PU 14234) from the earliest Palaeocene (Puercan) of Mantua lentil of Wyoming.

The anterior opening of the infraorbital canal is 2.08 mm high and located above the mesiolabial root of P3. In this respect *Simoclaenus* differs from the condition in *Maiorana* and *Baioconodon*, in which the infraorbital foramen is located more posteriorly, above the mesiolabial root of P4. A condition similar to that of *Maiorana* and *Baioconodon* is observed in *Didolodus multicuspis* (MACN 10690), in which the infraorbital foramen is located above the distal edge of P3 and most of the P4 (Gelfo, personal communication). Anterior to this foramen is a tiny opening located above the anterior root of P2, and which probably represents a nutrient foramen. In its anterior region, the maxilla is not inflated laterally by the canine as is observed in *Alcidedorbignya*, due to the fact that the canine was compressed transversely. This condition particularly resembles the "condylarths" of Mantua lentil of Wyoming, *Baioconodon* and *Maiorana*.

The third specimen referred to *Simoclaenus sylvaticus* is a partial maxilla with M1-2 (MHNC 13876), (Fig. 9). The M2 perfectly matches the size and morphology of that of MHNC 8348 described by Muizon & Cifelli (2000). The small differences between the two teeth are the presence, in MHNC 13876, of a slightly larger parastyle, a cuspule on the preparaconular crista located between the paraconule and the parastyle and a slight inflation of the lingual end of the precingulum (cuspule?). The M2 of MHNC 13876 has the characteristic asymmetrical morphology observed in *Molinodus* and *Simoclaenus*, in which the paracone is distinctly more labial than the metacone (Muizon & Cifelli 2000: fig. 2A-C, fig. 14C). This condition is not observed on the M1 of *Molinodus*, the paracone of which is not shifted labially. The most interesting characteristic of this specimen is in the relative wear stage of the M2 and M1. The M2 has a wear stage approximately similar to that of the M2 of MHNC 8348. In contrast the M1 is totally excavated in its lingual two thirds: the protocone, the protocristae and the conules, the pre-and postcingula, and the trigon basin have disappeared; the only preserved elements of the tooth are the para- and metacones, the styles and the labial cingulum. This wear stage is clearly more advanced than that observed on the M1 of MHNC 8348, in which the protocone and conules are coalescent but still identifiable, the protocristae and the pre-and postcingula are distinctly observable. This stage of wear of M2-1 of MHNC 8348 is comparable to that observed on the maxilla of *Molinodus suarezi* (MHNC 1247) described by Muizon & Cifelli (2000). In fact, the extensive wear of the M1 of MHNC 13876 is comparable to the condition that could be observed on a DP4, an interpretation impossible given the fact that the posterior tooth is undoubtedly an M2, which presents the characteristic asymmetrical morphology of that tooth (Muizon & Cifelli 2000). Furthermore, the roots of the M1 are long and the lingual root perforates the floor of the orbit, which suggests that it is not a deciduous molar.

In ventral view, laterally to M2, the maxillar process of the zygoma and the anterior border of the orbitotemporal fossa are preserved. The latter is at the level of the apex of the metacone of M2, while it is at the level of the paracone of M3 on the maxilla (MHNC 8348) referred to *Simoclaenus* by Muizon & Cifelli (2000). In *Molinodus* the anterior edge of the orbitotemporal fossa is at the level of the paracone of M3 and in *Baioconodon* (YPM-PU 14234) and *Maiorana* (YPM-PU 16667 and 14171) it is at the level of the metacone of M3. However, this condition is likely to be individually variable since in *Alcidedorbignya inopinata* out of 13 specimens, in which it can be observed, three of them (see Muizon *et al.* 2015: fig. 10B) have an anterior edge of the orbitotemporal fossa at the level of the metacone of M2, as observed in the *Simoclaenus* specimen described here. In the other ten specimens, the anterior edge of the fossa is at the level of the paracone of M3. In the *Alcidedorbignya*

sample the anterior position of M2 is observed in young adults and may be related to the ontogenetic increase of the length of the rostrum.

Tiuclaenus minutus Muizon & Marshall, 1987

Diagnosis. — See Muizon & Cifelli (2000).

Description

A maxilla with M1-3 (MHNC 13879) is referred to *Tiuclaenus minutus*. It bears three almost unworn molars, and has been referred to this species essentially on the basis of its size (Fig. 10A). *Tiuclaenus minutus* is the smallest "condylarth" species of the Tiupampa fauna and the molars of the new specimen are even slightly smaller than those of MHNC 1240 described by Muizon & Cifelli (2000: fig. 7C). For example, the length of the molar row is 5.86 mm in MHNC 13879, while it is 6.74 mm on MHNC 1240, but such a size difference is likely related to individual variation. The size and proportions of the upper molar of this specimen depart from the other species of *Tiuclaenus* and from *Pucanodus*, which are distinctly larger (see Muizon & Cifelli 2000: tables 7-9). However, some slight morphological differences exist between the specimens referred to *T. minutus*, which differ in the larger size of the para- and metastyles, the para-and metacones more approximated, the more pronounced ectoflexus and labial cingulum. Nevertheless, in spite of these morphological differences we tentatively refer MHNC 13879 to *T. minutus*, considering that they could regarded as related to individual variation, an interpretation that could be revised when a larger sample of that species will be available.

Tiuclaenus robustus Muizon & Cifelli, 2000

Diagnosis. — See Muizon & Cifelli (2000).

Description

A right mandible fragment bearing m2-3 (MHNC 13875) has been referred to *Tiuclaenus robustus* (Fig. 10B, C) essentially because, although structurally similar to the other species of *Tiuclaenus* (*T. minutus* and *T. cotasi*), it differs from them in its size, distinctly larger, and in its greater massiveness. Furthermore, as is observed on the holotype (a mandible fragment with m2-m3, MHNC 1233), m3 of MHNC 13875 is proportionally shorter than in *T. minutus* and *T. cotasi* being barely longer than m2. An interesting feature of this specimen is the morphology of the roots of m2 and m3, which are long extending ventrally on more than 2.5 the height of the crown (Fig. 10C). Furthermore, the apices of the roots are markedly splayed with their posterior edges extending posteriorly, providing the extremity of the root a characteristic hammer-shape. Although the ventral edge of the dentary is partly broken, this morphology gives the impression that the root had to develop posteriorly because it was abutting the ventral edge of the mandibular canal.

Pucanodus gagnieri Muizon & Marshall, 1991

Diagnosis. — See Muizon & Cifelli (2000).

Description

A mandible fragment bearing m2-3 (MHNC 13869) has been referred to *Pucanodus gagnieri* (Fig. 11) because it presents the mesiodistal compression of the molars especially m3, which is characteristic of that species (Muizon & Marshall 1991). The specimen is approximately of the size of a small *Tiuclaenus*. The teeth are almost unworn and better illustrate this taxon than the holotype (a mandible with p3-m3), the teeth of which, are notably worn. The massive proportions of the teeth (large width relative to length) and particularly the shortness of the talonid of m3 are conspicuous on this specimen. As in all kollpaniines and North American mioclaenines, the entoconid and hypoconulid are connate (almost confluent) and the talonid basin is an obliquely oriented groove open anterolingually.

Measurements are provided on Table 5.

DISCUSSION

Dental loci and specimen distribution

The description of several new specimens of "condylarths" from the early Palaeocene of Tiupampa (Bolivia), although it does not increment the taxonomic list of the fauna, significantly improves the knowledge of the dental anatomy of the kollpaniine mioclaenids (Table 6). These new data essentially concern the upper and/or lower premolars, the morphology of the protocone, the size difference between M1/m1 and M2/m2, and the morphology of the lateral process of the maxilla of *Simoclaenus*. Among others, the new specimens of *Simoclaenus sylvaticus* described here confirm the shortness of the rostrum of this taxon on the basis of the vertical implantation of P1/p1, the mesiodistal shortness of p4, and the supposedly subvertical premaxilla-maxilla suture on the anterior region of the rostrum. In this respect, *S. sylvaticus* differs from *Molinodus suarezi*, in which p1 is procumbent, and p4 is not compressed mesiodistally, being much longer than wide.

The total number of "condylarths" specimens with addition of the new specimens recovered since the review of Muizon & Cifelli (2000) reaches 89 specimens, which represents a significant source of data given the age of the Tiupampa fauna (early Danian). The abundance and jaw distribution of the specimens according to taxa is presented in Table 7.

Premolars

The mandible MHNC 13867 which bears p3-m3 provides an indication that the p4 referred to *Molinodus* by Muizon & Cifelli (2000: fig. 3 M, N) may not belong to this species. The newly described p4 of *Molinodus* (Fig. 2) is not anteroposteriorly compressed with a metaconid lingual to the protoconid, but is more slender, longer and narrower, and has a metaconid distolingual to the protoconid.

FIG. 10. — **A**, *Tiuclaenus minutus*: partial right maxilla of with M1-3 (MHNC 13879), stereophotograph of occlusal view; **B**, *Tiuclaenus robustus*: partial right mandible with m2-3 (MHNC 13875), stereophotograph of occlusal view; **C**, the same in labial view. Scale bar: 5 mm.

FIG. 11. — *Pucanodus gagnieri*: partial right mandible with m2-3 (MHNC 13869): **A**, stereophotograph of occlusal view; **B**, the same in labial view. Scale bar: 5 mm.

Furthermore, a maxilla with a complete series of upper premolars is referred to *Simoclaenus sylvaticus* (Fig. 8). The upper premolars of *S. sylvaticus* present a well-developed protocone on P3-4 (protocone of P3 is almost as developed as that of P4) and an incipiently developed protocone on P2 (just an inflation of the posterolingual angle of the tooth, a protoconal bulge, not individualized as a distinct cusp as on the posterior premolars). Although the P1 and P2 of *Molinodus suarezi* are unknown, the P3 of this taxon exhibits a large protocone as in *S. sylvaticus*. It is likely that the P1 and P2 of *M. suarezi* were similar to those of *S. sylvaticus*.

Based on the condition observed on the middle-late Jurassic eutherian *Juramaia sinensis* (Luo *et al.* 2011), on the oetlestids *Prokennalestes trofimovi* and *P. minor* (Kielan-Jaworowska & Dashzeveg 1989), on the zhelestids *Parazhelestes robustus* and *Aspanlestes aptap* (Nessov *et al.* 1998; Archibald & Averianov 2005) and on the cimolestid *Puercolestes simpsoni* (Williamson *et al.* 2011), the plesiomorphic condition in eutherians would be a poorly-developed protocone on P3 or penultimate upper premolar (either a simple bulge or a very small cusp on the distolingual edge of P3) and a well-developed protocone (almost as large as the paracone) on P4. Therefore, *Molinodus* and *Simoclaenus* are clearly derived in this respect. They are more derived than the North American mioclaenid, *Promioclaenus acolytus* (e.g., USNM 9575, AMNH 32728) as well as the earliest Palaeocene (Mantuan) *Baioconodon nordicum* (YPM-PU 14234), in which the protocone is well-developed on P4, incipient on P3 and absent on P2 (CM personal observations). However, the condition of the P3 protocone may represent a labile and homoplastic feature since a well-individualized protocone is present in some (but not all) specimens of *Oxyprimus galadrielae* (PU 21015) and in *Maiorana noctiluca* (PU 16667) from the basal Puercan of Mantua hills (Wyoming) as well as in *Promioclaenus lemuroides* (AMNH 4025). Furthermore, it is noteworthy that a well-developed protocone on P3 is also present in *Zalambdalestes*, *Asioryctes* and *Kennalestes* from the late Cretaceous of Mongolia (Kielan-Jaworowska 1981; Wible *et al.* 2004).

Among the other Tiupampa kollpaniines the upper premolars are known in *Tiuclaenus cotasi*, *T. robustus*, and *Pucano-*

TABLE 5. — Measurements of the kollpaniine specimens described in text (in mm).

Taxon and Tooth	Body part	No. spec.	Length	Width	Trig width	Tal width	Others
Molinodus suarezi	c	MHNC 13883	2.44	1.75	–	–	–
	p1	MHNC 13883	1.56	1.23	–	–	–
	roots p2	MHNC 13883	2.59	–	–	–	–
	p3	MHNC 13867	3.18	1.94	–	–	–
	p4	MHNC 13867	3.23	2.03	–	–	–
	m1	MHNC 13867	3.29	–	2.20	1.99	–
	m2	MHNC 13867	3.83	–	2.71	2.60	–
	m3	MHNC 13867	4.71	–	2.71	2.39	–
Height of dentary below m2	dentary	MHNC 13867	–	–	–	–	7.13
Simocalenus sylvaticus	roots p2	MHNC 13872	2.42	–	–	–	–
	roots p3	MHNC 13872	2.77	–	–	–	–
	p4	MHNC 13872	2.97	2.84	–	–	–
	m1	MHNC 13872	3.58	–	3.03	2.67	–
	root C	MHNC 13868	3.94	2.45	–	–	–
	P1	MHNC 13868	1.99	1.40	–	–	–
	P2	MHNC 13868	2.66	2.03	–	–	–
	P3	MHNC 13868	3.35	3.56	–	–	–
	P4	MHNC 13868	3.17	3.98	–	–	–
Height of Maxilla at level of infraorbital foramen	Maxilla	MHNC 13868	–	–	–	–	12.14
	M1	MHNC 13876	3.36	4.47	–	–	–
	M2	MHNC 13876	3.74	6.11	–	–	–
Tiuclaenus minutus	M1	MHNC 13879	2.20	3.10	–	–	–
	M2	MHNC 13879	2.23	3.45	–	–	–
	M3	MHNC 13879	1.54	2.87	–	–	–
Length M1-3	M1-3	MHNC 13879	–	–	–	–	5.86
Tiuclaenus robustus	m2	MHNC 13875	3.64	–	3.04	2.64	–
	m3	MHNC 13875	3.71	–	2.52	2.14	–
Pucanodus gagnieri	m2	MHNC 13869	2.92	–	2.47	2.28	–
	m3	MHNC 13869	3.23	–	2.84	1.99	–

dus gagnieri (Muizon & Cifelli 2000: fig. 8A, 10G, 11B). The condition in these taxa differs from that of *Molinodus* and *Simoclaenus* since the protocone of P3 is significantly smaller than that of P4 and P2 in *T. cotasi* (P2 is unknown in *T. robustus* and *P. gagnieri*) has no protoconal bulge. Therefore, according to the plesiomorphic condition of zhelestids and cimolestids, *Tiuclaenus* and *Pucanodus* exhibit a less derived condition than *Molinodus* and *Simoclaenus*.

Among other South American "condylarths" (e.g., Didolodontidae) a well-developed protocone is present on the P3-4 of the Casamayoran highly derived species *Didolodus multicuspis* (MACN 10690), but it is poorly developed on the P3 of the Itaboraian taxon *Ricardocifellia protocenica* (Paula Couto 1952a: pl. 32, fig. 1). Furthermore, in early litopterns from Itaboraí (i.e. Protolipternidae), the protocone of P3 is distinctly smaller than on P4 in *Protolipterna ellipsodontoides* (MCT-1495M) and possibly in *Miguelsoria parayirunhor*. In the latter, P3-4 are unknown but the specimen MNRJ 4094V, a maxilla with the three molars and a P2 with a protoconal bulge, presents the alveoli of P3-4, which are distinctly three-rooted, with the lingual root (receiving the protocone) of P3 conspicuously smaller than that of P4. This condition strongly suggests a P3 with a distinctly smaller protocone than on P4. The P3 lacks a well-developed protocone in *Asmithwoodwardia scotti* (Paula Couto 1952a: pl. 33 fig. 3). However, comparison is made difficult because a complete set of upper premolars is unknown in many early didolodontids (including the Peligran taxa *Escribania* and *Raulvaccia*). Pending more data are known on those taxa, the condition of *Simoclaenus* and *Molinodus* is regarded as probably more derived than that of most North and South American Palaeocene "condylarths", since they exhibit a greater specialization in the process of development

TABLE 6. — Dental loci known so far in the Tiupampa kollpaniines. Abbreviations: **al**, alveolus; **low**, lower teeth; **rt**, roots; **T**, tooth; **up**, upper teeth. New data from the specimens described in this paper are marked in red.

	I1	I2	I3	C	P1	P2	P3	P4	M1	M2	M3
Molinodus suarezi											
up	–	–	–	–	–	–	T	T	T	T	T
low	al	al	al	T	T	T	T	T	T	T	T
Simoclaenus sylvaticus											
up	–	–	–	rt	T	T	T	T	T	T	T
low	–	–	–	–	al	rt	rt	T	T	T	T
Tiuclaenus minutus											
up	–	–	–	–	–	–	–	–	T	T	T
low	–	T	al	T	al	T	T	T	T	T	T
Tiuclaenus cotasi											
up	–	–	–	–	–	T	T	T	T	T	T
low	–	–	–	–	–	–	T	T	T	T	T
Tiuclaenus robustus											
up	–	–	–	–	–	–	T	T	T	T	T
low	–	–	–	–	–	T	–	–	T	T	T
Pucanodus gagnieri											
up	–	–	–	–	–	–	T	T	T	T	T
low	al	al	al	T	rt	T	T	T	T	T	T
Andinodus boliviensis											
up	–	–	–	–	–	–	–	–	–	–	–
low	–	–	–	–	–	–	–	–	–	T	T

TABLE 7. — Distribution of kollpaniine specimens from Tiupampa according to taxa.

Number of specimens	Total number	Upper jaws	Isolated upper teeth	Lower jaws	Isolated lower teeth
Tiuclaenus cotasi	25	1	7	10	7
Molinodus suarezi	21	3	5	9	4
Tiuclaenus minutus	15	5	4	4	2
Pucanodus gagneri	15	3	8	4	–
Tiuclaenus robustus	6	1	2	2	1
Simoclaenus sylvaticus	5	3	–	2	–
Andinodus boliviensis	2	–	–	2	–

of the protocone of the premolars. In contrast, other Tiupampa kollpaniines (*Tiucalenus* and *Pucanodus*) more closely resemble in this respect the North American mioclaenids and early South American didolodontids and litopterns. Among other South American Native Ungulates (SANU) the early notoungulate *Henricosbornia lophodonta* (MACN 10808) and the basal astrapothere *Eoastrapostylops riolorense* also have a P3 with a distinctly smaller protocone than on P4. The P2 of *E. riolorense* (P2 unknown in *H. lophodonta*) lacks a protoconal bulge as in *Tiuclaenus.*

PROTOCONE, HYPOCONE, AND PSEUDOHYPOCONE

One of the new specimens of *Molinodus suarezi* described here, is a maxilla, which bears the three molars (Fig. 5). Although the labial edge of M1-2 is damaged, the most interesting feature of this specimen rests on the protocone of these teeth. This cusp is clearly elongated anteroposteriorly (the wear facets are oval-shaped) and on M2 the apex of the cusp is clearly pinched transversely, individualizing an anterior and a posterior lobe, the latter being smaller than the former (Fig. 5). This condition had been already observed on *Molinodus* by Muizon & Cifelli (2000: fig. 2A) on the specimen MHNC 8280. This incipient process of duplication of the protocone is tentatively regarded here as an incipient process of individualization of a hypocone.

The hypocone is a newly acquired cusp of the tribosphenic molar, which tends to enlarge the occlusal area of the tooth distolingually. The acquisition of a hypoconal cusp in mammals is a heavily homoplastic apomorphy, which occurred at least 20 times in mammalian evolution (Hunter & Jernvall 1995). It is most commonly achieved in two main different ways (Hershkovitz 1971; Hunter & Jernvall 1995; Jernvall 1995; Gheerbrant *et al.* 2016):

1) The postcingulum develops a lingual cusp, which increases in size and reaches that of the protocone. It is the hypocone of Hershkovitz (1971) also frequently called "true" hypocone (e.g., Stehlin 1916; Gregory 1922; Voruz 1970; Hunter & Jernvall 1995; Anemone *et al.* 2012). In this case, the increase in size of the postcingulum features a transitional stage called hypocone shelf (Jernvall 1995). A "true" hypocone (postcingulum-derived hypocone) has been documented, for example in phenacodontids and perissodactyls (Gheerbrant *et al.* 2016; but see below for a possible alternative interpretation of the perissodactyls hypocone), in the South American didolodont "condylarths" *Escribania* (Gelfo *et al.* 2007), *Ricardocifellia*, *Didolodus*, in the protolipternid litopterns *Miguelsoria*, *Protolipterna*, *Asmithwoodwardia*, and in, at least, some other litopterns (e.g., *Licaphrium*, *Picturotherium*), (personal observations). In these taxa, the hypocone does not represent a posterior extension of the protocone. The postprotocrista still connects the protocone to the metaconule and the latter has no connection with the hypocone thus demonstrating that the hypocone is actually an enlarged post-cingular cusp, and therefore a true hypocone. Furthermore, the protocone and the hypocone are fully separated up to the base of the cusps, thus retaining the initial separation of the postcingulum and the protocone.

2) The second frequently observed pattern of formation of a hypocone is not a cusp neoformation but is achieved by a distolingual migration of the metaconule, which increases in size posterior to the protocone. This type of hypocone (metaconule-derived hypocone) has been called pseudohypocone (e.g., Ladevèze *et al.* 2010; Gheerbrant *et al.* 2016). This condition is observed for instance in Paenungulatomorpha (Gheerbrant *et al.* 2016), Artiodactyla (Hunter & Jernvall 1995), and pleuraspidotheriid "condylarths" (Ladevèze *et al.* 2010).

If one designates a postcingulum derived (see above) as the "true" hypocone, following for instance Stehlin (1916), Gregory (1922), and Butler 2000, then functional hypocones of other origins are *de facto* pseudohypocones. The term "pseudohypocone" has been created by Stehlin (1916) to designate the cusp arising from a postprotocone fold on the posterior edge of the protocone (the "*Nannopithex* fold"), possibly homologous to part of the postprotocrista (Godinot 2007) (but see Hershkovitz [1977] and Anemone *et al.* [2012] for a different interpretation). This third pattern of formation of a functional hypocone is present in notharctine primates (e.g., Gregory 1920, 1922; Gazin 1958; Butler 2000; Anemone *et al.* 2012). All other primates have a true hypocone (i.e. postcingulum-derived). A pseudohypocone derived from the posterior extension of the protocone posterior slope has also been documented (in addition to notharctines) for Dinocerata (Wheeler 1961; Hunter & Jernvall 1995; Jernvall 1995). In these taxa, however, the pseudohypocone results from a budding of the posterior slope of the protocone rather than from a duplication of the protocone. Based on these considerations, three main types of functional hypocones formation are distinguished here and designated as follows (though other modes may exist; Hunter & Jernvall 1995): the postcingulum-derived "true" hypocone, the metaconular (M) pseudohypocone and the protocone-derived pseudohypocone, either derived from a posterior extension of the protocone posterior slope (PPSD) or derived from a duplication of the whole protocone (PDD).

The condition observed in *Molinodus suarezi* foreshadows the protocone-duplication-derived (PDD) pattern of individualization of a pseudohypocone. Such a PDD pseudohypocone may also be present in *Raulvaccia peligrensis* (from the early Palaeocene of Punta Peligro). In this taxon (Gelfo 2007: fig. 2C, D), the distolingual cusp is still connate to the

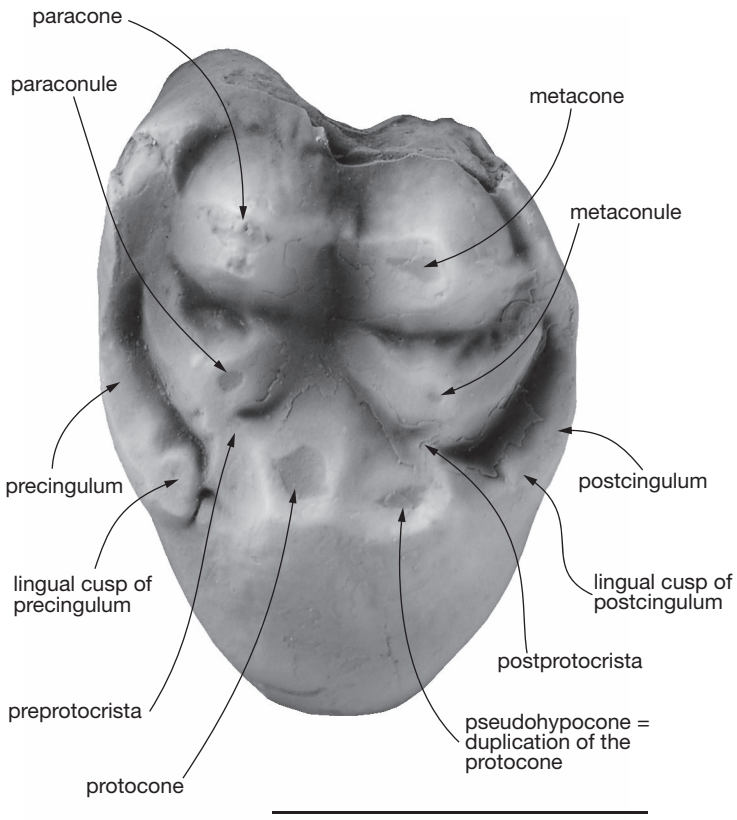

Fig. 12. — *Raulvaccia peligrensis*: left M2 (cast of MLP 90-II-12-70) in occlusal view. Comment: we tentatively refer this tooth to an M2 (*contra* Gelfo 2007, who refers it to an M1?) because of the mesiolabial position of the paracone (as related to metacone), which provides to the tooth a distinct asymmetrical morphology as is observed on the M2s of *Molinodus* and *Simoclaenus* but not on the M1s of these taxa. Scale bar: 5 mm.

distal edge of the protocone (the tooth being triangular and not quadrate) and is well separated from the distal cingulum (which bears a distinct small lingual cusp, indicating its lingual end – see Fig. 12 and Gelfo 2007: fig. 2C, D) and much higher, a condition which suggests a process of duplication from the protocone similar to that observed in *Molinodus*. The condition of *Raulvacia* is more similar to what is observed in *Molinodus* than to that of the M2 of *Escribania* (MLP 90-II-12-63) figured by (Gelfo *et al.* 2007: fig. 4e), in which the two cusps appear to be well individualized, separated by a deep lingual furrow (absent in *Raulvacia* and *Molinodus*), and not connate all along their length in contrast to the condition observed in *Molinodus*. Furthermore, in *Raulvacia*, the cusp distal and connate to the protocone (pseudohypocone), is still attached to the metaconule by a postprotocrista, which would suggest that it originates from a duplication of the protocone and not from the postcingulum. This condition further suggests that the distolingual cusp of the M2 of *Raulvacia* actually represents a PDD pseudohypocone (Fig. 12). Such a condition is not observed on the M2 of *Escribania* mentioned above. Furthermore, the latter tooth is associated (on a maxillary fragment) to an M3, which presents a well-individualized protocone and no well-defined hypocone but a distally inflated postcingulum whose lingual cusp is clearly lower than the protocone. This condition would indicate that the increase of the crushing surface of the tooth, in *Escribania*, is achieved through the postcingulum rather than through a duplication of the protocone. An almost identical condition is also observed on MNRJ 1462-V a maxilla fragment of *Ricardocifellia protocenica* bearing right M2-3. On this specimen (whose teeth are better preserved than those of *Raulvacia peligrensis* considered above), M2 has a distinctly postcingulum-derived-hypocone (with a protocone connected to metaconule by the postprotocrista, and a hypocone not connected to metaconule), whereas M3 has no hypocone but a thickened postcingulum. It is noteworthy, however, that *Raulvaccia* differs from *Molinodus* (and *Lamegoia;* see below) in the lingual edge of the postcingulum, which reaches the apex of the cusp connate to the protocone, whereas, in the latter two genera, it remains at the base of the cusp.

The oval-shaped morphology observed on the protocone of the M2 referred to *Simoclaenus sylvaticus* described above (Fig. 9), probably indicates, in this taxon, a pattern similar to that of *Molinodus* and, possibly, *Raulvacia*.

As mentioned by Muizon & Cifelli (2000: 73), a condition indicating a pattern similar to that of *Molinodus*, but more emphasized, is present on an unworn M2 referred by Paula Couto (1952a: pl. 32, fig. 7) to *Lamegoia conodonta* (paratype, MNRJ 1465-V). On this specimen (Fig. 13B), the protocone is partly divided into two cusps, which are confluent on most of their height and whose apices only are fully separated. The mesial cusp is connected to the paraconule by a short oblique

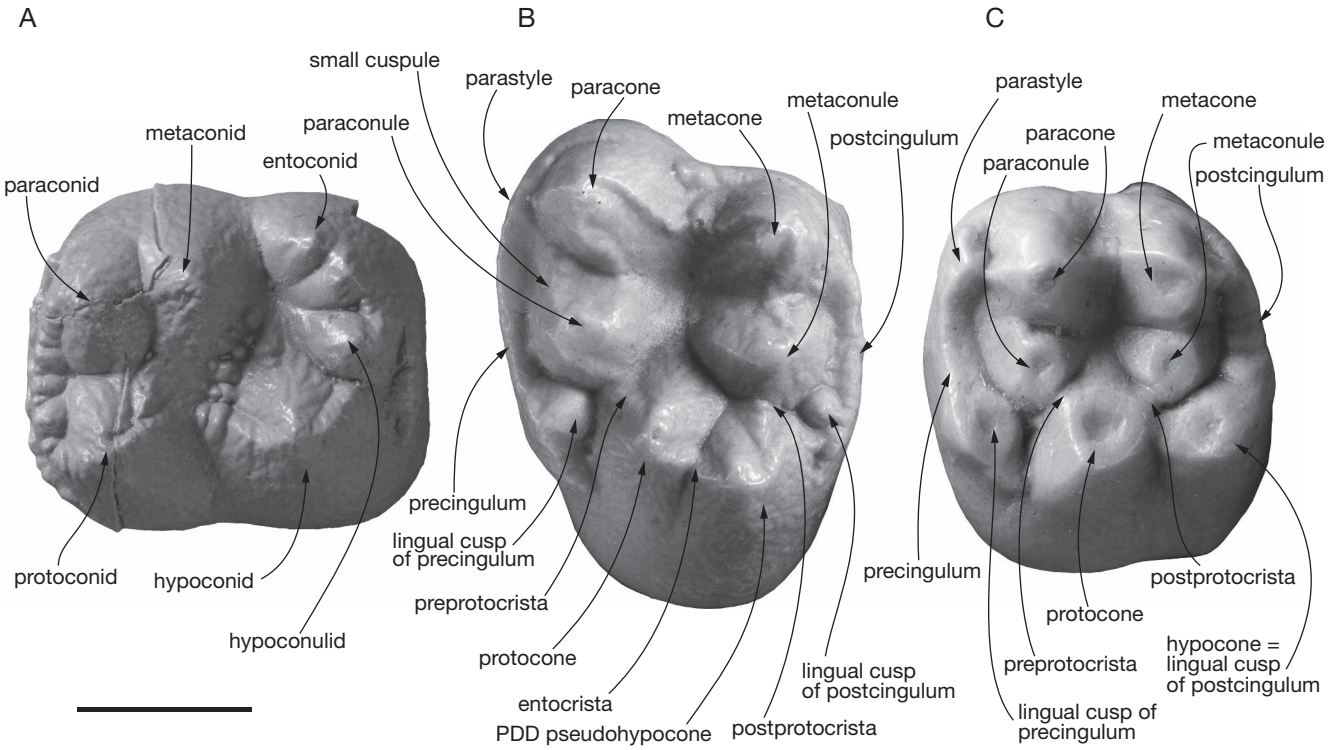

FIG. 13. — **A**, **B**, *Lamegoia conodonta*; **C**, didolodontidae indet.; **A**, occlusal view of a left m2 of *Lamegoia conodonta* (cast of holotype MNRJ 1463-V); **B**, occlusal view of a right M2 (reversed) of *Lamegoia conodonta* (cast of MNRJ 1465-V); **C**, occlusal view of a left M2 (cast of MNRJ 1464-V) of and undetermined didolodont (referred by Paula Couto [1952a] to *L. conodonta*). Scale bar: 5 mm.

preprotocrista and the posterior cusp is connected to the metaconule by a short transverse crista, which we interpret as the postprotocrista. The postcingulum presents a small lingual cusp which contacts both the distal protoconal cusp and the metaconule at their base. The distal cusp of the protocone of the M2 of *Lamegoia* mentioned above is regarded here as a PDD pseudohypocone in process of individualization. The other molar referred by Paula Couto (1952a: pl. 32, fig. 8), (paratype MNRJ 1464-V) bears a true hypocone, which is clearly the enlargement of the lingual cusp of the postcingulum (Fig. 13C). This hypocone is not connected to the metaconule and the postprotocrista links the metaconule to the protocone. In contrast, the hypocone of MNRJ 1465-V is connected to the protocone by an anteroposteriorly oriented short crista (the entocrista of Hershkovitz 1971), whereas such a structure is absent in MNRJ 1464-V. We therefore conclude that the two upper molars referred by Paula Couto (1952a) to *Lamegoia conodonta*, exhibit a different pattern of formation of a hypocone, and are probably not referable to the same taxon. Now, because the holotype of *L. conodonta* is an isolated lower molar (Fig. 13A), it is unclear what tooth actually represents an upper molar of *L. conodonta*, if any. However, the *Molinodus*-like molar (MNRJ 1465-V) presents a finely wrinkled enamel and its cristae are granulous as if they were formed of adjoined little cuspules (Fig. 13B). This morphology perfectly matches the condition observed on the lower molar of the holotype but distinctly differs from the other upper molar (with a true hypocone). Furthermore, as noted by Jernvall (1995), the development of a hypocone (distolingual cusp) and the consecutive squaring of the upper molars is associated to a reduction of the paraconid (mesiolingual cusp). Because the paraconid of the holotype of *Lamegoia conodonta* is not reduced (in contrast to the condition in *Miguelsoria*, which has squared upper molars with a large true hypocone) this condition could be related to a lesser development of a posterolingual cusp (i.e. a PDD pseudohypocone still connate to the protocone). Therefore, we tentatively refer the molar with a PDD pseudohypocone (MNRJ 1465-V) to the holotype of *L. conodonta*. The other molar (MNRJ 1464-V), with a true postcingulum-derived hypocone better resembles a large didolodontid close to *Ricardocifellia* (personal observations).

The upper molar (M2, MNRJ 1465-V) referred here to *Lamegoia conodonta* (Fig. 13B) also resembles the M2s of *Molinodus* and *Simoclaenus* in its asymmetrical (roughly triangular) outline as mentioned by Muizon & Cifelli (2000: 73). This morphology is in part due to the size and position of the paracone, which is larger than the metacone and placed more labially. Interestingly, the M2 of *L. conodonta* bears a small cuspule between the paraconule and the small parastyle. A similar cuspule is also observed on the unworn M2 of *Molinodus suarezi* (Muizon & Cifelli 2000: fig. 2A) and also on the new M2 of *Simoclaenus sylvaticus* described above (Fig. 9). Such a cuspule is not observed or is barely discernible on the other South American "condylarths" or protolipternids. An asymmetrical, roughly triangular, outline of the M2 is also observed in *Raulvaccia* from Punta Peligro (Gelfo 2007: fig. 4C).

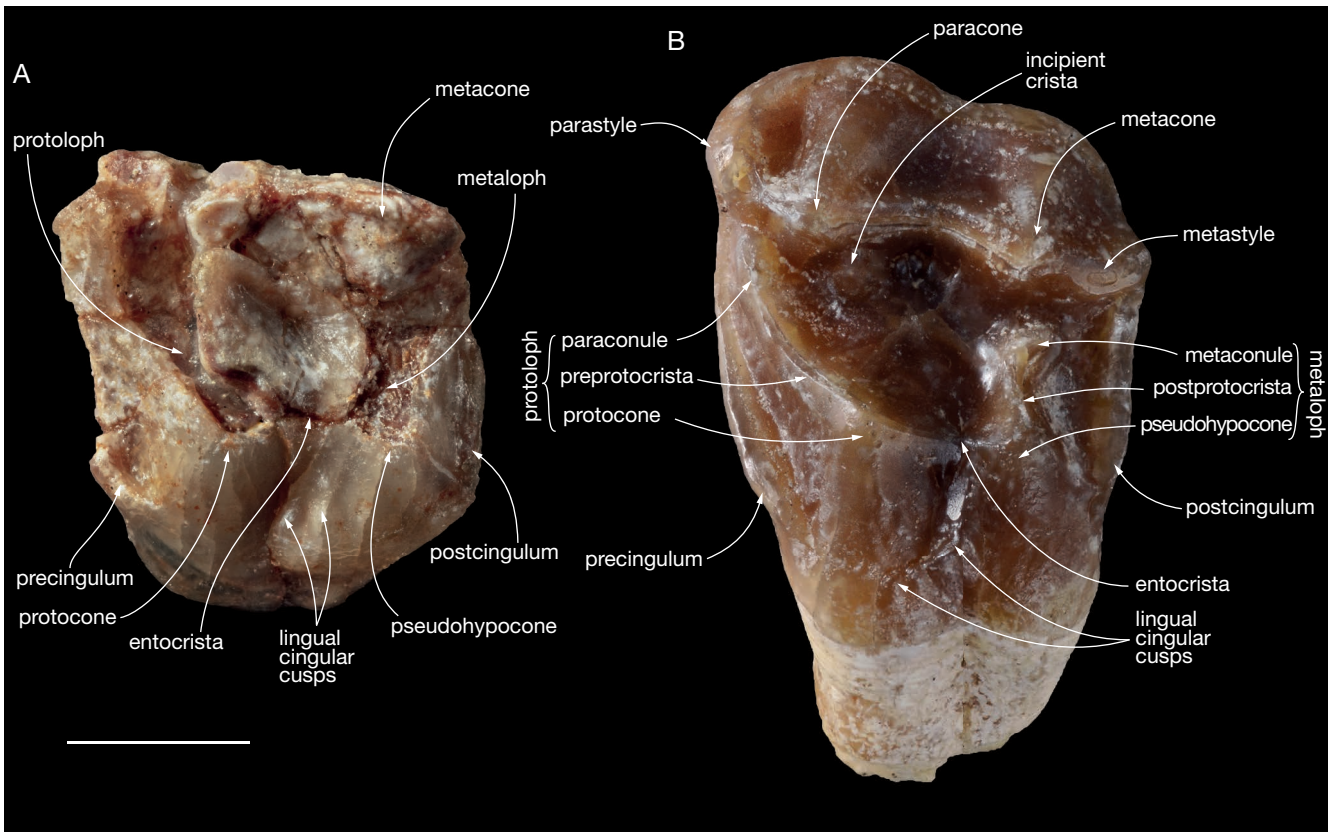

Fig. 14. — Notoungulates left upper molars (M1 or M2) in occlusal view: **A**, MNHN VIL 123, the only notoungulate tooth from Tiupampa (cf. Henricosborniidae); **B**, MNHN.F.CAS2714, cf. *Henricosbornia*. Scale bar: 5 mm.

We have not observed any other M2 of "condylarths" in South America which matches those aspects of the M2 of *Molinodus* and *Simoclaenus* as well as those of *Lamegoia conodonta* and *Raulvaccia peligrensis*. Furthermore, the m2 (holotype) of *L. conodonta* (Fig. 13A) resembles the m2 of *Molinodus* (Figs 4; 5) in its large paraconid, probably related to the posteriorly displaced metaconid and to the obliquity of the protocristid. This condition is not present in *Didolodus*, *Asmithwoodwardia*, and *Protolipterna*; it is present, to a lesser extent, in *Ricardocifellia*, *Ernestokokenia*, and *Miguelsoria*.

Among other SANUs, a pseudohypocone resulting from the duplication of the protocone may also be present in notoungulates. The oldest notoungulate record is represented by an isolated incomplete upper molar from Tiupampa (Muizon *et al.* 1984; Muizon 1992), (Fig. 14A). The tooth, although damaged, distinctly presents the characteristic features of the basal notoungulate pattern illustrated by the upper molar of cf. *Henricosbornia* (MNHN.F.CAS2714; Fig. 14B) (Simpson 1948; Cifelli 1993; Billet 2011). On both teeth, the protoloph and metaloph respectively bear at their lingual edges the protocone and the pseudohypocone. We regard the latter as a pseudohypocone for the following reasons: 1) because of the presence of a crest (postprotocrista) that connects it to the metaconule (worn off on the Tiupampa specimen), embedded within the metaloph; 2) because of the position of the lingual edge of the postcingulum, which remains at base of the pseudohypocone not presenting any lingual cusp nor any connection to the pseudhypocone; and 3) because of the lack of crista connecting the protocone to the metaconule (Fig. 14B). Similar observations were also made on other early diverging notoungulates such as *Colbertia* and *Simpsonotus* (pers. obs.). Because of this configuration, it is unlikely that the posterolingual cusp of the notoungulate molar could be derived from the increase in size of the lingual end of the postcingulum as is observed for a true hypocone (e.g., in protolipternids, didolodontids, phenacodontids) (*contra* Hunter & Jernvall 1995: table 1, who identified the hypocone of notoungulates as postcingulum-derived). In both figured notoungulate specimens, the protocone and pseudohypocone are linked by a distinct entocrista, a condition that is never as pronounced in didolodontids and litopterns. If this interpretation is correct, the molar structure of *Molinodus* (as well as that of *Lamegoia*) would more resemble, in this respect, the notoungulate than the litoptern pattern. This hypothesis may favor an inclusion of the Notoungulata in the Panameriungulata in a position closer to the Kollpaniinae than to the Litopterna. Such a position for notoungulates has already been suggested by Cifelli (1993), who stated that they could readily have derived from a *Tiuclaenus*-like ancestral morphotype. Furthermore, Cifelli's statement has been reinforced by the similarities between the tarsus of *Tiuclaenus* and early diverging notoungulates (Muizon *et al.* 1998; Muizon & Cifelli 2000). Therefore, the assumed similar pattern of pseudohypocone formation in some kollpaniines (*Molinodus*, *Simoclaenus*), *Lamegoia*, and, possibly,

TABLE 8. — Taxa, specimens and references concerning the section "Molar proportions in kollpaniines and other 'ungulates'".

Taxa/Observation	Specimen no.	Measurements (mm)				Data Source (GB measurement unless specified otherwise)
		M2/M1	M3/M1	m2/m1	m3/m1	
Zalambdalestes lechei	PSS-MAE 130	0.857	0.485	–	–	Wible *et al.* (2004: fig. 9, table 2)
Maelestes gobiensis	PSS-MAE 607	1.083	0.710	–	–	Wible *et al.* (2009: figs and text, table 1)
Prokennalestes trofimovi	GI-PST material	1.067	0.709	–	–	Kielan-Jaworowska & Dashzeveg (1989: fig. 1)
Kennalestes gobiensis	Z. Pal. No. MgM-I/2	1.162	0.808	–	–	Cast of Z. Pal. No. MgM-I/2 and Kielan-Jaworowska & Dashzeveg (1989: fig. 2, pl. 24)
Leptictis dakotensis	YPM-PU 16232 (& MCZ-VP:19678)	1.013	0.560	–	–	Morphobank media number M132552 & M132528
Altacreodus magnus	UALVP 3793	1.003	0.644	–	–	Fox (2015: fig. 1A, B)
Didelphodus absarokae	USGS 3951	1.055	0.611	–	–	Casts of USGS 5972 and 3951
Puercolestes simpsoni	UCMP 33658	1.052	0.817	–	–	Cast of UCMP 36658
Pararyctes pattersoni	UM 80855	1.123	0.703	–	–	Cast of UM 80855
Molinodus suarezi	YPFB Pal 6112	1.280	1.120	1.278	1.119	–
Molinodus suarezi	MHNC 13867	1.530	1.620	1.526	1.619	–
Molinodus suarezi	MHNC 13870	1.506	1.036	–	–	–
Simoclaenus sylvaticus	MHNC 13876	1.616	-	–	–	–
Simoclaenus sylvaticus	MHNC 8332	1.320	1.270	1.322	1.272	–
Simoclaenus sylvaticus	MHNC 8348	1.631	1.187	–	–	–
Tiuclaenus minutus	MHNC 13879	1.186	0.652	–	–	–
Tiuclaenus minutus	MHNC 1240	1.297	0.748	–	–	–
Tiuclaenus minutus	YPFB Pal 6115	1.230	1.330	1.232	1.327	–
Tiuclaenus cotasi	MHNC1231	1.240	1.130	1.240	1.132	–
Pucanodus gagnieri	MHNC 8343	1.200	0.758	–	–	–
Pucanodus gagnieri	MHNC 1239	1.120	1.090	1.124	1.087	–
Protungulatum donae	UM5206	1.508	0.886	–	–	Cast of UM5206
Didolodus multicuspis	MACN A10690	1.161	0.974	–	–	Cast of MACN A10690
Ernestokokenia cf. *nitida*	MNHN.F.CAS681	1.220	1.420	1.224	1.424	–
Pleuraspidotherium aumonieri	MNHN.F.BR17498	1.240	0.939	–	–	–
Arctocyon primaevus	Berru L-15 (MNHN.F)	1.117	0.540	–	–	–
Phenacodus primaevus	USNM V 20068	1.058	0.849	–	–	Cast of USNM V 20068
Ocepeia daouiensis	MNHN.F.PM54	1.128	1.065	–	–	Gheerbrant *et al.* (2014: fig. 10B)
Chriacus pelvidens	UNSM 2949	1.381	0.930	–	–	Cast of USNM 2949
Hyopsodus minusculus	AMNH 12493	1.157	0.744	–	–	Cast of AMNH 12493
Hyopsodus miticulus	YPM-PU 16164	1.206	0.608	–	–	Cast of PU 16164
Maiorana noctiluca	YPM-PU 16667	1.269	0.892	–	–	Cast of YPM-PU 16667
Mimatuta minuial	YPM-PU 16702	1.340	0.941	–	–	Cast of YPM-PU 16702
Oxyprimus galadrielae	YPM-PU 16866	1.193	0.617	–	–	Cast of YPM-PU 16866
Promioclaenus aquilonius	AMNH 35728	1.264	0.610	–	–	Cast of AMNH 35728
Promioclaenus lemuroides	AMNH 4025	1.182	0.583	–	–	Cast of AMNH 4025
Anthracobune wardi	RR-411	1.325	1.252	–	–	Cooper *et al.* (2014)
Kalitherium marinus	IITR/SB/VLM 931	1.627	1.452	–	–	Bajpai *et al.* (2006)
Abdounodus hamdii	MHNM.KHG.154	1.209	0.883	–	–	Gheerbrant *et al.* (2016: fig. 1)
Teilhardimys brisswalteri	MNHN.F.CR265-Bn	1.105	0.499	–	–	Hooker & Russell (2012: fig. 26)
Periptychus carinidens	NMMNH P-19482	1.118	0.824	–	–	Shelley *et al.* (2018: fig. 3)
Simpsonotus praecursor	MLP 73-VII-3–11	1.093	0.804	–	–	Cast of MLP 73-VII-3–11
Notostylops murinus	MNHN.F.CAS96	1.008	0.706	–	–	–
Isotemnus sp.	MNHN.F.CAS372	1.046	0.771	–	–	–
Oldfieldthomasia sp.	MNHN.F.CAS393 (and AMNH 28678)	1.109	0.925	–	–	–
Ultrapithecus rutilans	MNHN.F.CAS387	1.066	0.968	–	–	–
Notopithecus adapinus	MNHN.F.CAS1039 (and AMNH 28949)	1.052	0.779	–	–	–
Henricosbornia lophodonta	MACN 10808	1.049	0.950	–	–	Cast of MACN 10808
Colbertia magellanica	AMNH 49873	1.436	1.134	–	–	Cast of AMNH 49873
Trigonostylops wortmanni	MNHN.F.CAS187	1.338	1.289	–	–	–
Miguelsoria parayirunhor	MNRJ 4094	1.521	1.224	–	–	Cast of MNRJ 4094
Diadiaphorus majusculus	MNHN.F.SCZ207	1.060	0.658	–	–	–
Proterotherium australe	MNHN.F.SCZ205	1.106	0.784	–	–	–
Asmithwoodwardia scotti	DGM-358-M	1.070	0.743	–	–	Cast of DGM-358M
Acotherulum saturninum	MNHN.F.Qu16366	1.083	0.828	–	–	–
Dichobune sp.	MNHN.F.Qu16586	1.074	0.791	–	–	–
Metriotherium mirabile	MNHN.F.Qu82	1.143	1.021	–	–	–
Diacodexis pakistanensis	HGSP 300 5003	1.328	1.183	–	–	Thewissen *et al.* (1983: fig. 1a)

TABLE 8. — Continuation.

Taxa/Observation	Specimen no.	Measurements (mm)				Data Source (GB measurement unless specified otherwise)
		M2/M1	M3/M1	m2/m1	m3/m1	
Doliochoerus quercyi	MNHN.F.Qu5	1.230	1.148	–	–	–
Cebochoerus sp.	MNHN.F.Qu2003	1.112	0.972	–	–	–
Cainotherium sp.	MNHN.F.Qu1833	1.361	1.320	–	–	–
Dacrytherium ovinum	MNHN.F.Qu168	1.247	1.232	–	–	–
Anoplotherium commune	MNHN.F.Qu377	1.244	1.334	–	–	–
Vigugna vigugna	MNHN-ZM-AC-1957-1034	0.970	0.857	–	–	–
Lama glama	MNHN-ZM-AC-1897-488	1.241	1.010	–	–	–
Camelus bactrianus	MNHN-ZM-AC-1962-183	1.320	1.113	–	–	–
Camelus dromedarius	MNHN-ZM-AC-1852-564	1.286	1.269	–	–	–
Tayassu pecari	MNHN-ZM-AC-2013-1320	1.311	1.261	–	–	–
Babyrousa babyrussa	MNHN-ZM-AC-1993-4617	1.677	1.956	–	–	–
Hylochoerus meinertzhageni	MNHN-ZM-AC-1998-1792	1.841	2.457	–	–	–
Pecari tajacu	MNHN-ZM-AC-1981-439	1.338	1.328	–	–	–
Potamochoerus porcus	MNHN-ZM-AC-2007-1467	1.417	1.675	–	–	–
Sus scrofa	MNHN-ZM-AC-2013-1210	1.580	1.882	–	–	–
Cervus elaphus	MNHN-ZM-AC-1890-4032	1.216	1.235	–	–	–
Muntiacus muntjac	MNHN-ZM-AC-1962-4182	1.326	1.318	–	–	–
Muntiacus sp.	MNHN-ZM-AC-1900-610	1.191	1.024	–	–	–
Odocoileus hemonius	MNHN-ZM-AC-AE 722	1.198	0.968	–	–	–
Cervus nippon	MNHN-ZM-AC-1967-278	1.381	1.459	–	–	–
Rucervus eldii	MNHN-ZM-AC-1908-146	1.410	1.399	–	–	–
Elaphurus davidianus	MNHN-ZM-AC-1974-96	1.157	1.215	–	–	–
Rangifer tarandus	MNHN-ZM-AC-1909-85.1	1.148	0.944	–	–	–
Rangifer tarandus	MNHN-ZM-AC-1909-85.2	1.079	0.863	–	–	–
Alces sp.	MNHN-ZM-AC-1979-49	1.195	1.052	–	–	–
Hydropotes inermis	MNHN-ZM-AC-1971-37	1.132	0.955	–	–	–
Blastocerus dichotomus	MNHN-ZM-AC- ssN	1.228	1.095	–	–	–
Moschiola memina	MNHN-ZM-AC-1967-934	1.322	1.162	–	–	–
Hyemoschus aquaticus	MNHN-ZM-AC-1969-471	1.407	1.358	–	–	–
Rusa timorensis	MNHN-ZM-AC-1927-44	1.400	1.386	–	–	–
Rusa unicolor	MNHN-ZM-AC-1884-543	1.343	1.352	–	–	–
Rusa unicolor	MNHN-ZM-AC-1919-46	1.312	1.328	–	–	–
Pudu puda	MNHN-ZM-AC-2000-144	1.122	0.885	–	–	–
Dama mesopotamica	MNHN-ZM-AC-2009-237	1.084	0.956	–	–	–
Mazama gouazoubira	MNHN-ZM-AC-1982-796	1.197	1.126	–	–	–
Mazama gouazoubira	MNHN-ZM-AC-1981-687	1.206	1.068	–	–	–
Mazama americana	MNHN-ZM-AC-1854-135	1.277	1.063	–	–	–
Mazama americana	MNHN-ZM-AC-I-2233	1.368	1.249	–	–	–
Hippocamelus bisulcus	MNHN-ZM-AC-1874-733	1.339	1.404	–	–	–
Capreolus capreolus	GB coll.	1.082	0.989	–	–	–
Litocranius walleri	MNHN-ZM-AC-1972-440	1.193	1.041	–	–	–
Tragelaphus angasii	MNHN-ZM-AC-1988-129	1.266	1.291	–	–	–
Giraffa camelopardis	MNHN-ZM-AC-1934-63	1.242	1.079	–	–	–
Okapia johnstoni	MNHN-ZM-AC-1978-27	1.076	1.030	–	–	–
Choeropsis liberiensis	MNHN-ZM-AC-1988-12	1.411	1.235	–	–	–
Hippopotamus amphibius	MNHN-ZM-AC-A2215	1.406	1.308	–	–	–
Anisodon grande	MNHN.F.Sa9339	1.645	1.699	–	–	–
Hyracotherium angustidens	AMNH 48018	1.289	1.160	–	–	Kitts (1956: fig. 1)
Palaeotherium sp.	MNHN.F.Qu7440	1.120	1.027	–	–	–
Pachynolophus lavocati	MNHN.F.Qu7371	1.274	1.334	–	–	–
Diceros bicornis	MNHN-ZM-AC-1961-195	0.943	0.628	–	–	–
Rhinoceros sondaicus	MNHN-ZM-AC-1932-48	1.055	0.677	–	–	–
Rhinoceros unicornis	MNHN-ZM-AC-2009-400	0.993	0.667	–	–	–
Tapirus terrestris	MNHN-ZM-AC-1928-287	1.274	1.130	–	–	–
Tapirus pinchaque	MNHN-ZM-AC-1982-034	1.163	1.165	–	–	–
Tapirus indicus	MNHN-ZM-AC-1944-267	1.245	1.444	–	–	–

notoungulates, again, could suggest phylogenetic affinities. It is noteworthy, however, that this pattern of pseudohypocone formation could be a homoplastic character shared by panameriungulates and notoungulates. Among other kollpaniines, a duplication of the protocone is not as conspicuous in *Tiuclaenus* and *Pucanodus*. However, on the M1 and M2 of MHNC 13879 (Fig. 10), a maxilla referred to *Tiuclaenus minutus*, the oval-shaped morphology of the wear facet at the apex of the protocone suggests that a similar duplication of the cusp may be incipient (see also Muizon & Cifelli 2000: fig. 7C). A similar condition is observed in *Pucanodus gagneri* (Muizon & Cifelli 2000: fig. 11).

It is noteworthy that a similar pattern of pseudohypocone formation may also be present in most perissodactyls ([The-

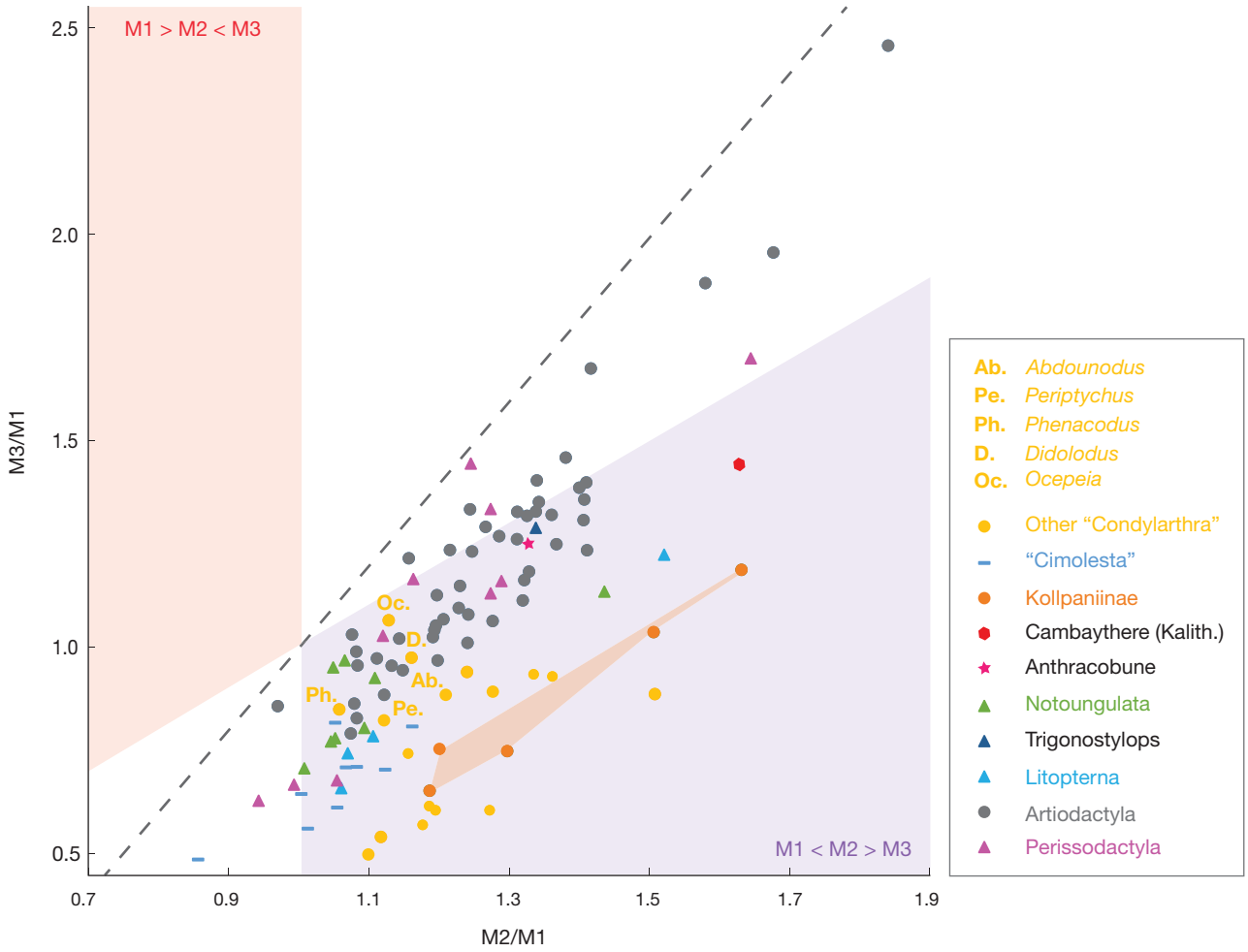

FIG. 15. — Upper molar proportions in Euungulata, "Condylarthra", SANUs, and the kollpaniines from Tiupampa described here. Molar proportions are plotted in the developmental 'morphospace' (Kavanagh *et al.* 2007; Polly 2007) where the white region is consistent with the IC model; the broken line is the relationship predicted for lower molar of murine rodents (see Material and methods and Table 8). Abbreviations: **Kalith.**, *Kalitherium*.

nius 1989], but *contra* Gheerbrant *et al.* [2016], who regard the perissodactyl hypocone as a true, cingulum-derived, hypocone) (note: "perissodactyls" refers here to the "perissodactyla *sensu stricto*" of Rose *et al.* 2014). As abundantly discussed and illustrated by Thenius (1989) and Hooker (1989, 1994), the morphology of the protoloph and metaloph of perissodactyls can be observed in early diverging members of the clade (e.g., in Equoidea, Brontotheroidea, Ancylopoda, Tapiroidea, Rhinocerotoidea). They are respectively formed by the paraconule and metaconule labially and by the protocone and the pseudohypocone (called hypocone by Thenius 1989 and Hooker 1994) lingually. Although many authors regard the hypocone of perissodactyls as a true hypocone (e.g., Hunter & Jernvall 1995; Holbrook 2015), the lingual cusp of the metaloph may also well be a protocone-derived pseudohypocone since in early perissodactyls (e.g., *Hyracotherium*, *Hallensia*, *Propachynolophus*, *Pliolophus*) the distolingual cusp of upper molars is well separated from the well-developed postcingulum but is linked to the metaconule by a robust crest (postprotocrista?) and the protocone lacks distinct connection to the metaconule (thus resembling the condition observed in *Lamegoia*, (Fig. 13B) and notoungulates, (Fig. 14B) (Hooker 1994; Bronnert *et al.* 2017). If the hypocone of perissodactyls is actually a PDD pseudohypocone, this pattern would be congruent with the recently advocated molecular-based relationships of notoungulates to perissodactyls (Welker *et al.* 2015; Westbury *et al.* 2017). However, the sister group relationship of notoungulates (PDD pseudohypocone) and litopterns (true hypocone) retrieved by Welker *et al.* (2015), both forming a clade with the other perissodactyls – ((notoungulates, litopterns) other perissodactyls) – would indicate that the origin and evolution of the posterolingual cusp of upper molars in perissodactyls is probably more complex and requires further studies.

Therefore, the *Molinodus*-like incipient pattern of pseudohypocone formation (derived from a duplication of the protocone) may probably be widely distributed among eutherian (e.g., in perissodactyls, including some South American relatives), whereas the development of metaconule-derived pseudohypocone (i.e. an enlarged and displaced metaconule) is abundantly present, for example, in artiodactyls and paenungulates (Gheerbrant *et al.* 2016; *contra* Hunter & Jernval 1995).

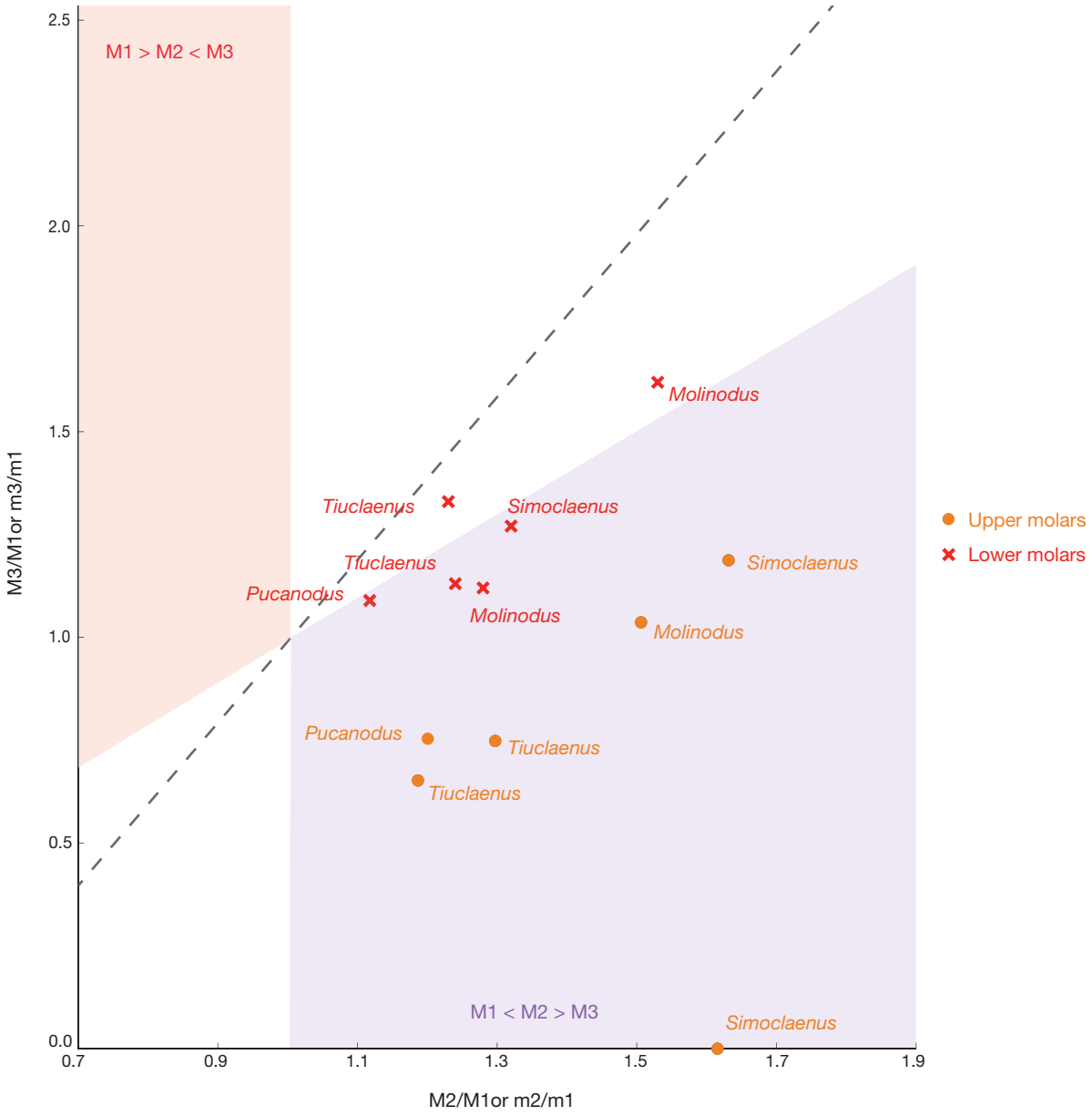

Fig. 16. — Upper and lower molar proportions in kollpaniines from Tiupampa. Molar proportions are plotted in the developmental 'morphospace' (Kavanagh *et al.* 2007; Polly 2007) where the white region is consistent with the IC model; the broken line is the relationship predicted for lower molar of murine rodents (see Material and methods and Table 8). The specimen of *Simoclaenus* placed on the horizontal axis corresponds to MHNC 13876, for which the M3 is not preserved.

Molar proportions in kollpaniines and other "ungulates"

As mentioned above, the smaller size of M1/m1 relative to the second molar is a characteristic of the Tiupampa kollpaniines. Therefore, in order to analyze this feature, we have characterized the molar proportions of kollpaniines, with the ratios of molar areas (M2/M1 and M3/M1, m2/m1 and m3/m1), and have plotted them on two graphs following previous studies (e.g., Kavanagh *et al.* 2007; Polly 2007; Halliday & Goswami 2013; Gomes-Rodrigues *et al.* 2017) (Figs 15, 16; Table 8). We have also plotted several other taxa of "condylarths", as well as euungulates.

On graph of Fig. 15, kollpaniines are found in a separate area of the morphospace together with many other "condylarths" (e.g., *Arctocyon*, *Maiorana*, *Protungulatum*). These taxa share similar molar proportions where the M2 is by far the largest molar (Fig. 15). Cimolestans and litopterns are found at an intermediate position between kollpaniines and artiodactyls, perissodactyls and notoungulates, which are shifted towards a relatively smaller M2. It is worth noting however that almost all sampled taxa, except for some artiodactyls and perissodactyls, are found in the area where M2 is the largest molar. Kollpaniines and many "condylarths" are thus found in an area of the morphospace that is distinctly separated from most euungulates (Artiodactyla, Perissodactyla, Notoungulata and Litopterna) and from taxa traditionally included within Cimolesta (serving as an outgroup here). A few "condylarths" (e.g., *Didolodus*, *Phenacodus*) or ungulate-like taxa are found

closer to euungulates than to kollpaniines and other "condylarths" (e.g., *Arctocyon*, *Maiorana*, *Protungulatum*). This is the case of African ungulate-like taxa (*Ocepeia* and, to a lesser degree, *Abdounodus*), which are regarded as early diverging paenungulatomorphs (Gheerbrant *et al.* 2016) and therefore may represent a placental offshoot totally different from many "condylarths" known on the northern continents.

The very large second molar, relatively to other molars, which characterizes many "condylarths" is not restricted to upper molars. The situation is indeed somewhat similar for lower molars in kollpaniines, though to a lesser extent (Fig. 16). Only the lower molar proportions observed in one *Tiuclaenus* and one *Molinodus* specimen fall within the area predicted by the model of Kavanagh *et al.* (2007). For other kollpaniines, m2 is the largest molar, but size ratios for lower molars are shifted towards a relatively less large second molar when compared to the condition in upper molars. Interestingly, Halliday & Goswami (2013) have previously shown that many taxa traditionally included within "Condylarthra" (and Acreodi) also exhibit unusually large lower m2 relative to the size of both m1 and m3, which distinguishes them from many other placental taxa. This is particularly intriguing since these taxa fall in an area of the morphospace unpredicted by the Inhibitory Cascade Model of Kavanagh *et al.* (2007). This model, which was originally proposed for lower molars in murine rodents, states that the relative size of the molars may be governed by a rather simple developmental rule regulated by activator and inhibitor molecules during the sequence of molar formation (Kavanagh *et al.* 2007). It predicts that the second molar will generally have a size that is one-third of the combined size of all the three molars (Polly 2007). For lower molars, many "condylarths" fall outside the predictions made by this model, as shown by Halliday & Goswami (2013). Although the IC model may apply differently to upper molars (see Gomes-Rodrigues *et al.* 2017), it is worth noting that a direct transposition of this model to upper molars would show that many "condylarths" and kollpaniines again fall in an area very distant from the predicted zone, as evidenced in the present study (Fig. 15). Clade-specific differences in relative molar sizes were previously found in bears relative to other carnivorans (Polly 2007) and also among anthropoid primates (Carter & Worthington 2016), with cercopithecines showing values similar to many "condylarths" with relatively large m2. Carter & Worthington (2016) mentioned a frugivorous diet as a possible driver of these particular molar proportions in cercopithecines, whereas Halliday & Goswami (2013) mentioned a relatively wide dietary spectrum (omnivorous to herbivorous) as potentially linked to similar proportions in "condylarths". It is currently unclear if and how functional factors can explain these peculiar molar proportions. These require an early arrest of M3 development and a decrease in inhibition (Kavanagh *et al.* 2007; Polly 2007). It is intriguing to find these particularities shared by some "condylarths" (e.g., *Arctocyon*, *Maiorana*, *Protungulatum*) and kollpaniines, as "Condylarthra" is now viewed as a 'wastebasket taxon' (Shelley *et al.* 2018) and the many "condylarths" sharing relatively large M2 and m2 in our sample form a polyphyletic assemblage in recent detailed phylogenetic analyses (Halliday *et al.* 2017; Muizon *et al.* 2015). The 'M2 largest' condition exhibited by some "condylarths" (e.g., *Arctocyon*, *Maiorana*, *Protungulatum*) and kollpaniines from our sample is absent in many "cimolestan" taxa (Fig. 15), some of which are often viewed as stem placentals (Wible *et al.* 2009; Halliday *et al.* 2017). The 'm2 largest' condition, present in many "condylarths" and kollpaniines (this study and Halliday & Goswami 2013), is also absent in most placentals investigated for their lower molar proportions (Kavanagh *et al.* 2007; Polly 2007; Wilson *et al.* 2012; Halliday & Goswami 2013; Carter & Worthington 2016). For these reasons, the large size of both the upper and lower second molars relative to other molars may well represent a derived character state, which is shared, among a few others, by some "condylarths" and kollpaniines. It is questionable whether or not these derived molar proportions can be viewed as the sign of shared ancestry between those taxa, because close relationships between them were not supported by any recent study. However, the potential close relationships between some "condylarths" and perissodactyls on one side (Halliday *et al.* 2017), the proposed relationships between the latter and South American native ungulates (the Panperissodactyla hypothesis including notoungulates and litopterns; Welker *et al.* 2015; Westbury *et al.* 2017) and the possible affinities of kollpaniines to notoungulates and litopterns (Muizon & Cifelli 2000) on the other side, certainly make it worth analyzing the peculiar molar proportions shared by many Palaeocene South American kollpaniines and northern "condylarths". The possibility that this derived character may have been shared by potential early diverging euungulates or panperissodactyls, such as many "condylarths" and kollpaniines, before being erased by subsequent evolution in more recent members of these clades (Perissodactyla, Notoungulata, Litopterna), certainly deserves further investigation.

SUMMARY AND CONCLUSIONS

The new specimens described here, although not critical to the understanding of the origin and early radiation South American ungulates, significantly improve the knowledge of the dental and cranial anatomy of the earliest known South American ungulates, the Kollpaniinae (Panameriungulata, Mioclaenidae). The best represented species in the new sample are *Molinodus suarezi* and *Simoclaenus sylvaticus*. The *Molinodus* specimens provide information on the anterior region of the head. Although the incisors of this taxon are still unknown, their alveoli indicate that the incisor row was parabolic to V-shaped and the staggered condition of the i2, reveals some transverse compression of the mandibular symphysis (Fig. 1). These two features indicate that the apex of the snout was rather pointed and narrow. This assumption is reinforced by the procumbent p1 observed on the anterior mandibular fragment described above which could indicates an elongated rostrum or, at least, not shortened. The new

partial mandible (Fig. 2) is the most complete specimen known so far for *M. suarezi* and, because it bears p3-m3, it allows secure referral of lower premolars to *Molinodus*, the holotype of which is a mandible with m1-m3 (Muizon & Marshall 1987). The morphology of the newly referred premolars, that are transversely narrow and mesiodistally elongated, indicates that the mesiodistally compressed p4 referred by Muizon & Cifelli (2000) to *Molinodus* probably belong to another taxon.

Furthermore, on the two partial mandibles referred to *Molinodus suarezi* (Fig. 3), the coronoid crest and fossa are respectively very salient and deep. Similar development of these structures is also observed on the other partial mandibles described by Muizon & Cifelli (2000). The coronoid crest receives the insertion of the temporalis muscle; the deep coronoid fossa probably received the molar part of the buccinator muscle, the action of which is to return the food from the vestibulum to the masticatory surface of the teeth (Evans & de Lahunta 2013). The strong temporalis suggests powerful adductions of the mandible and the well-developed buccinator could indicate the need for a prolonged mastication. These muscular features associated to the robust bunodont molars of *M. suarezi*, may indicate some durophagous feeding items, such as large seeds or hard-shelled nuts.

The new maxilla of *Molinodus* (Figs 4; 5; 6), confirms the morphology of the protocone of M1 and M2. On both molars, the protocone is distinctly mesiodistally elongated and features an incipient process of duplication on M2. The wear of the enamel on this tooth conspicuously displays the presence of two well-formed cusps on the Enamel-Dentine Junction (EDJ). As shown by Anemone *et al.* (2012) the EDJ can be thought to preserve the first stage of crown development, in which the cusps and crests appear. We therefore conclude that *Molinodus suarezi* displays an incipient development of a distolingual cusp on its upper molar crown. The hypocone is initially derived from the enlargement of the lingual cusp of the postcingulum (true hypocone). Therefore, the posterior part of the duplicated protocone of *Molinodus*, is not a true hypocone but an incipient pseudohypocone. In this taxon, the presence of crest joining the pseudohypocone to the metaconule is the postprotocrista. A condition similar to *Molinodus* has been observed in *Lamegoia* (Fig. 13B) and possibly in *Raulvaccia* (Fig. 12). In these taxa, the distolingual cusp of the M2 is still connected to the metaconule by what we interpret as the postprotocrista, and is therefore regarded as a pseudohypocone.

This pattern of individualization of a distolingual cusp on upper molars (hypocone or pseudohypocone) is not commonly recorded with certitude among mammals. The most usual pattern of formation of a distolingual cusp is the enlargement of the lingual cusp of the post cingulum, and is commonly regarded as the true hypocone. In this case, the protocone is still connected to the metaconule by the prosprotocrista whereas the hypocone has no crest connection to it. This pattern is present in a large number of eutherians. The other distolingual cusps of the tribosphenic molar are pseudohypocone. Three of them can be recorded: 1) the *Molinodus-Lamegoia* duplication of the protocone as mentioned above; 2) a budding from the posterior slope of the protocone as is observed in notharctine primates and dinocerates; and 3) the enlargement and distolingual migration of the metaconule, which occurs in artiodactyls, pleuraspidotheriid "condylarths", paenungulates, some carnivores, and most metatherians in which a distolingual cusp is present. In fact, this third pseudohypocone, should not be called as such (although many authors do so), since it is does not represent a true neoformation, this cusp being still the metaconule.

Among South American native ungulates (SANUs), litopterns and didolodonts (Fig. 13C) are clearly featuring a true hypocone (but see condition in *Raulvaccia*). Condition in astrapotheres, pyrotheres, and xenungulates is unresolved. However, we have suggested a *Molinodus*-like pattern of protocone-derived pseudohypocone in notoungulates on the basis of the morphology observed in the earliest members of the order, especially the presence of a crest (postprotocrista) joining the pseudohypocone to the metaconule (Fig. 14). Nevertheless, it is clear that more data on the hypocone formation are needed in early diverging members of SANU clades especially based on the observation of the surface of the dentine at the enamel dentine junction.

It is noteworthy, however, that, whatever the pattern, the development of a functional hypocone is remarkably widespread among tribosphenic mammals and therefore represents a highly homoplastic character, especially the true hypocone, which is apparently the most common, but still requires further investigation.

The new *Simoclaenus* specimens are not abundant but provide a welcome confirmation on the cranial anatomy of this poorly known kollpaniine. The anterior mandible fragment bearing p4-m1 (Fig. 7) confirms the mesiodistal compression of the lower premolars in this taxon. Furthermore, the almost complete lateral ascending process of the maxilla bearing P1-4 confirms the rostrum shortness of this kollpaniine (Fig. 8). The vertical P1 (p1 is also vertical on the mandible), the subvertical premaxilla-maxilla suture, and the elevated and erected lateral wall of the maxilla also confirm the shortness of the snout suggested by Muizon & Cifelli (2000). Although *Simoclaenus* is phylogenetically close to *Molinodus*, the two genera clearly differ in the morphology of their snout which was probably significantly shorter in the former.

The study of molar proportions in kollpaniines from Tiupampa, and the comparison with euungulates and ungulate-like taxa, reveals an intriguing characteristic worthy of further investigation. In kollpaniines and many "condylarths", the M2 and m2 are much larger than the other upper and lower molars respectively, a pattern not found in the artiodactyls, perissodactyls and SANUs examined. The peculiar molar proportions shared by kollpaniines and many condylarths also depart from the predictions of the IC model. It remains to be determined whether this unusual pattern could constitute evidence for shared ancestry among a subset of ungulate-like mammals.

Acknowledgements
The specimens described here have been collected during field expeditions funded by the National Geographic Society (grants 6296/98, 7109/01, 9394/13); Funds for fieldwork were also provided by the Muséum national d'Histoire naturelle (Paris, France), in 2006 and 2012. Fossil collecting was carried out under the auspices of research agreements between the Museo de Historia Natural Alcide d'Orbigny of Cochabamba (Bolivia) and the Muséum national d'Histoire naturelle (France). All the specimens collected are the property of the MHNC and were provided on loan to the MNHN for curation and publication. Field expeditions have benefited of logistical support from the IDR (Institut de Recherche pour le Développement) in Bolivia. We thank our Bolivian colleague Ricardo Céspedes-Paz, for his collaboration and logistic support during all the field seasons. Special thanks are due to Richard Cifelli (Oklahoma Museum of Natural History) and Javier Gelfo (Museo de La Plata) for providing cast of didolodontids and protolipternids. This work has benefited from fruitful discussion with Constance Bronnert, Emmanuel Gheerbrant, Marc Godinot, Grégoire Métais (CR2P, CNRS, MNHN, Sorbonne Université). Special thanks are due to Javier Gelfo and Lilian Bergqvist, whose careful reviews allowed for substantial improvement of our manuscript. Photographs were made by Philippe Loubry and Lilian Cazes.

REFERENCES

Anemone R. L., Skinner M. M. & Dirks W. 2012. — Are there two distinct types of hypocone in Eocene primates? The 'pseudohypocone' of notharctines revisited. *Palaeontologia electronica* 15 (3): 26A, 13 p.

Archibald J. D. & Averianov A. O. 2005. — Mammalian faunal succession in the Cretaceous of the Kyzylkum Desert. *Journal of Mammalian Evolution* 12: 9-22. https://doi.org/10.1007/s10914-005-4867-3

Asher R. & Helgen K. 2010. Nomenclature and placental mammal phylogeny. *BMC Evolutionary Biology* 10:102-110. https://doi.org/10.1186/1471-2148-10-102

Bai B., Wang Y-Q., Li Q., Wang H.-B., Mao F.-Y., Gong Y.-X. & Meng J. 2018. — Biostratigraphy and Diversity of Paleogene Perissodactyls from the Erlian Basin of Inner Mongolia, China. *American Museum Novitates* 3914: 1-60. https://doi.org/10.1206/3914.1

Bajpai S., Kapur V. V., Thewissen J. G. M., Das D. P. & Tiwari B. N. 2006. — New early Eocene cambaythere (Perissodactyla, Mammalia) from the Vastan Lignite Mine (Gujarat, India) and an evaluation of cambaythere relationships. *Journal of the Palaeontological Society of India* 51 (1): 101-110.

Billet G. 2011. — Phylogeny of the Notoungulata (Mammalia) based on cranial and dental characters. *Journal of Systematic Palaeontology* 9 (4): 481-497. https://doi.org/10.1080/14772019.2010.528456

Bronnert C., Gheerbrant E., Godinot M. & Metais G. 2017. — A primitive perissodactyl (Mammalia) from the early Eocene of Le Quesnoy (MP7, France). *Historical Biology* 30 (1-2): 237-250. https://doi.org/10.1080/08912963.2017.1341502

Buckley M. 2015. — Ancient collagen reveals evolutionary history of the endemic South American 'ungulates'. *Proceedings of the Royal Society of London B: Biological Sciences* 282 (1806): 20142671. https://doi.org/10.1098/rspb.2014.2671

Butler P. 2000. — The evolution of tooth shape and tooth function in primates, *in* Teaford M., Smith M. & Ferguson M. (eds), *Development, Function and Evolution of Teeth*. Cambridge University Press, Cambridge: 201-211. https://doi.org/10.1017/CBO9780511542626.014

Carter K. E. & Worthington S. 2016. — The evolution of anthropoid molar proportions. *BMC Evolutionary Biology* **16**: 110. https://doi.org/10.1186/s12862-016-0673-5

Cifelli R. L. 1983. — The origin and affinities of the South American Condylarthra and early Tertiary Litopterna (Mammalia). *American Museum Novitates* 2772: 1-49. http://hdl.handle.net/2246/5256

Cifelli R. L. 1993. — The phylogeny of the native South American ungulates, *in* Szalay F. S., Novacek M. J. & McKenna M. C. (eds), *Mammal Phylogeny*. Vol. 2. *Placentals*. Springer Verlag, New York: 195-216.

Clyde W. C., Wilf P., Iglesias A., Slingerland R. L., Barnum T., Bijl P. K., Bralower T. J., Brinkhuis H., Comer E. E., Huber B. T., Ibañez-Mejia M., Jicha B. R., Krause J. M., Schueth J. D., Singer B. S., Raigemborn M. S, Schmitz M. D., Sluijs A. & Zamaloa M. D. C. 2014. – New age constraints for the Salamanca Formation and lower Río Chico Group in the western San Jorge Basin, Patagonia, Argentina: Implications for Cretaceous-Paleogene extinction recovery and land mammal age correlations. *Geological Society of America Bulletin* 126: 289-306. https://doi.org/10.1130/B30915.1

Cooper L. N., Seiffert E. R., Clementz M., Madar S. I., Bajpai S., Hussain S. T. & Thewissen J. G. M. 2014. — Anthracobunids from the Middle Eocene of India and Pakistan are stem Perissodactyls. *PLoS ONE* 9 (10): e109232. https://10.1371/journal.pone.0109232

Evans H. E. & de Lahunta A. 2013. — *Miller's Anatomy of the Dog*. Saunders, St Louis, 850 p.

Fox R. C. 2015. — A revision of the Late Cretaceous-Paleocene eutherian mammal *Cimolestes* Marsh, 1889. *Canadian Journal of Earth Sciences* 52: 1137-1149. https://doi.org/10.1139/cjes-2015-0113

Gazin C. L. 1958. — A review of the Middle and upper Eocene primates of North America. *Smithsonian Miscellaneous Collections* 136 (1): 1-112. https://biodiversitylibrary.org/page/26247219

Gelfo J. N. 2004. — A new South American mioclaenid (Mammalia, Ungulatomorpha) from the Tertiary of Patagonia, Argentina. *Ameghiniana* 41: 475-484.

Gelfo J. N. 2007. — The 'condylarth' *Raulvaccia peligrensis* (Mammalia, Didolodontidae) from the Paleocene of Patagonia, Argentina. *Journal of Vertebrate Paleontology* 27: 651-660. https://doi.org/10.1671/0272-4634(2007)27[651:TCRPMD]2.0.CO;2

Gelfo J. N. & Sigé B. 2011. — A new didolodontid mammal from the late Paleocene- earliest Eocene of Laguna Umayo, Peru. *Acta Paleontologica Polonica* 54 (4): 665-678. https://doi.org/10.4202/app.2010.0067

Gelfo J. N., Goin F. J., Woodburne M. O. & Muizon C. de 2009. — Biochronological relationships of the earliest South American Paleogene mammalian faunas. *Palaeontology* 52 (1): 251-269. https://doi.org/10.1111/j.1475-4983.2008.00835.x

Gelfo J. N., Ortiz-Jaureguizar E. & Rougier G. W. 2007. — New remains and species of the "Condylarth" genus *Escribania* (Mammalia, Didolodontidae) from the Paleocene of Patagonia, Argentina. *Transactions of the Royal Society of Edimburgh, Earth and Environmental Sciences* 98: 127-138. https://doi.org/10.1017/S1755691007006081

Gheerbrant E., Amaghzaz M., Bouya B., Goussard F., Letenneur C. 2014. — *Ocepeia* (Middle Paleocene of Morocco): the oldest skull of an afrotherian mammal. *PLoS ONE* 9: e89739. https://doi.org/10.1371/journal.pone.0089739

Gheerbrant E., Filippo A. & Schmitt A. 2016. — Convergence of Afrotherian and Laurasiatherian Ungulate-Like Mammals: First Morphological Evidence from the Paleocene of Morocco. *PLoS ONE* 11 (7): e0157556. https://doi.org/10.1371/journal.pone.0157556

GODINOT M. 2007. — Primate origins: a reappraisal of historical data favoring tupaiid affinities, *in* RAVOSA M. J. & DAGOSTO M. (eds), *Primates Origins: Adaptations and Evolution*. Springer verlag, New York: 83-142. https://doi.org/10.1007/978-0-387-33507-0_4

GOIN F. J., PASCUAL R., TEJEDOR M., GELFO J. N., WOODBURNE M., CASE J., REGUERO M., BOND M., CIONE A., UDRIZAR SAUTHIER D., BALARINO L., SCASSO R., MEDINA F. A. & UBALDÓN M. C. 2006. — The earliest Tertiary therian mammal from South America. *Journal of Vertebrate Paleontology* 26 (2): 505-510. https://doi.org/10.1671/0272-4634(2006)26[505:TETTMF]2.0.CO;2

GOMES-RODRIGUES E., HERREL A. & BILLET G. 2017. — Ontogenetic and life history trait changes associated with convergent ecological specializations in extinct ungulate mammals. *Proceeding of the national Academy of Science of the United States of America* https://doi.org/10.1073/pnas.1614029114

GREGORY W. K. 1920. — On the structure and relations of *Notharctus*, an American Eocene primate. *Memoirs of the American Museum of Natural History*, New series, Volume 3 (2): 1-243. https://biodiversitylibrary.org/item/165714

GREGORY W. K. 1922. — The origin and evolution of the human dentition. Williams and Wilkins, Baltimore, xviii p., 548 p., 15 pls.

HALLIDAY T. J. D. & GOSWAMI A. 2013. — Testing the inhibitory cascade model in Mesozoic and Cenozoic mammaliaformes. *BMC Evolutionary Biology* 13 (79): 1-11. https://doi.org/10.1186/1471-2148-13-79

HALLIDAY T. J., UPCHURCH P. & GOSWAMI A. 2017. — Resolving the relationships of Paleocene placental mammals. *Biological Reviews* 92 (1): 521-550. https://doi.org/10.1111/brv.12242

HERSHKOVITZ P. 1971. — Basic crown patterns and cusp homologies of mammalian teeth, *in* DAHLBERG A. A. (ed.), *Dental Morphology and Evolution*. University of Chicago Press, Chicago: 95-150.

HERSHKOVITZ P. 1977. — *Living New World Monkeys (Platyrrhini), with an Introduction to Primates*. Volume 1. University of Chicago Press, Chicago, 1132 p.

HERSHKOVITZ P. 1982. — The staggered marsupial lower third incisor (i3). *Geobios*, mémoire spécial, 6: 191-200. https://doi.org/10.1016/S0016-6995(82)80113-7

HERSHKOVITZ P. 1995. — The staggered marsupial lower incisor: hallmark of cohort Didelphimorphia. and description of a new genus and species with staggered i3 from the Albian (Lower Cretaceous) of Texas. *Bonner Zoologische Beitrage* 45 (3-4): 153-169. https://biodiversitylibrary.org/page/44799597

HOLBROOK L. 2015. — The identity and homology of the postprotocrista and its role in molarization of upper premolars of Perissodactyla (Mammalia). *Journal of Mammalian Evolution* 22: 259-269. https://doi.org/10.1007/s10914-014-9276-3

HOOKER J. J. 1989. — Character polarity in early perissodactyls and their significance for *Hyracotherium* and intraordinal relationships, *in* PROTHERO D. R. & SCHOCH R. M. (eds), *The Evolution of Perissodactyls*. Oxford University Press, New York: 79-101.

HOOKER J. J. 1994. — The beginning of the equoid radiation. *Zoological Journal of the Linnean Society* 112: 29-63. https://doi.org/10.1111/j.1096-3642.1994.tb00311.x

HOOKER J. J. & RUSSELL D. E. 2012. — Early Palaeogene Louisinidae (Macroscelidea, Mammalia), their relationships and north European diversity. *Zoological Journal of the Linnean Society* 164 (4): 856-936. https://doi.org/10.1111/j.1096-3642.2011.00787.x

HUNTER J. P. & JERNVALL J. 1995. — The hypocone as a key in mammalian evolution. *Proceeding of the National Academy of Sciences of the United States of America* 92: 10718-10722. https://doi.org/10.1073/pnas.92.23.10718

JERNVALL J. 1995. — Mammalian molar cusp pattern: developmental mechanisms of diversity. *Acta Zoologica Fennica* 198: 1-61.

KAVANAGH K. D., EVANS A. R. & JERNVALL J. 2007. — Predicting evolutionary patterns of mammalian teeth from development. *Nature* 449: 427-432. https://doi.org/10.1038/nature06153

KIELAN-JAWOROWSKA Z. 1981. — Evolution of the therian mammals in the Late Cretaceous of Asia. Part IV. Skull structure of *Kennalestes* and *Asioryctes*. *Palaeontologia Polonica* 42: 25-78.

KIELAN-JAWOROWSKA Z. & DASHZEVEG D. 1989. — Eutherian mammals from the Early Cretaceous of Mongolia. *Zoologica Scripta* 18 (2): 347-355. https://doi.org/10.1111/j.1463-6409.1989.tb00460.x

KITTS D. B. 1956. — American *Hyracotherium* (Perissodactyla, Equidae). *Bulletin of the American Museum of Natural History* 110 (1): 1-60.

KRAMARTZ A. G. & BOND M. 2005. — Los litopterna (Mammalia) de la Formación Pinturas, Mioceno Temprano-Medio de Patagonia. *Ameghiniana* 42 (3): 611-625.

LADEVÈZE S., MISSIAEN P. & SMITH T. 2010. — First skull of *Orthaspidotherium edwarsi* (Mammalia, "Condylarthra") from the late Paleocene of Berru (France) and phylogenetic affinities of the enigmatic European family Pleuraspidotheriidae. *Journal of Vertebrate Paleontology* 30 (5): 1559-1578. https://doi.org/10.1080/02724634.2010.501440

LUO Z.-X., YUAN C.-X., MENG Q.-J. & JI Q. 2011. — A Jurassic eutherian mammal and divergence of marsupials and placentals. *Nature* 476: 442-445. https://doi.org/10.1038/nature10291

MARSHALL L. G., SEMPERE T. & BUTLER R. F. 1997. — Chronostratigraphy of the mammal-bearing Palaeocene of South America. *Journal of South American Earth Sciences* 10: 49-70. https://doi.org/10.1016/S0895-9811(97)00005-9

MUIZON C. DE 1992. — La fauna de mamíferos de Tiupampa (Paleoceno inferior, Formacíon Santa Lucía) Bolivia. *Revista Técnica de Yacimientos Petrolíferos Fiscales de Bolivia* 12 (3-4): 575-624.

MUIZON C. DE & CIFELLI R. L. 2000. — The "condylarths" (archaic Ungulata, Mammalia) from the early Palaeocene of Tiupampa (Bolivia): implications on the origin of the South American ungulates. *Geodiversitas* 22 (1): 47-150.

MUIZON C. DE & MARSHALL L. G. 1987 — Le plus ancien Condylarthre (Mammalia) sud-américain (Crétacé supérieur, Bolivie). *Compte Rendus hebdomadaires des Séances de l'Académie des Sciences* 304: 771-774.

MUIZON C. DE & MARSHALL L. G. 1991. — Nouveaux Condylarthres du Paléocène inférieur de Tiupampa (Bolivie). *Bulletin du Muséum national d'Histoire naturelle*, *section C*, *Sciences de la Terre*, 4ème série, 13: 201-225. https://biodiversitylibrary.org/page/55803145

MUIZON C. DE, CIFELLI R. L. & BERGQVIST L. P. 1998. — Eutherian tarsals from the early Paleocene of Bolivia. *Journal of Vertebrate Paleontology* 18: 655-663. https://doi.org/10.1080/02724634.1998.10011092

MUIZON C. DE, MARSHALL L. G. & SIGÉ B. 1984. — The mammal fauna from the El Molino Formation (Late Cretaceous, Maestrichtian) at Tiupampa South Central Bolivia. *Bulletin du Muséum national d'Histoire naturelle*, *section C*, *Sciences de la Terre*, 4ème série, 6 (4): 327-351. https://biodiversitylibrary.org/page/55710289

MUIZON C. DE, BILLET G., ARGOT C., LADEVÈZE S. & GOUSSARD F. 2015. — *Alcidedorbignya inopinata*, a basal pantodont (Eutheria, Mammalia) from the early Palaeocene of Bolivia: anatomy, phylogeny, and palaeobiology. *Geodiversitas* 37 (4): 397-634. https://doi.org/10.5252/g2015n4a1

MUIZON C. DE, LADEVÈZE S., SELVA C., VIGNAUD R. & GOUSSARD F. 2018. — *Allqokirus australis* (Sparassodonta, Metatheria) from the early Palaeocene of Tiupampa (Bolivia) and the rise of the metatherian carnivorous radiation in South America. *Geodiversitas* 40 (16): 363-459. https://doi.org/10.5252/geodiversitas2018v40a16. http://geodiversitas.com/40/16

NESSOV L. A., ARCHIBALD J. D. & KIELAN-JAWOROWSKA Z. 1998. — Ungulate-like mammals from the Late Cretaceous of Uzbekistan and a phylogenetic analysis of Ungulatomorpha. *Bulletin of the Carnegie Museum of Natural History* 34: 40-88. https://biodiversitylibrary.org/page/52329844

PASCUAL R., VUCETICH M. G. & FERNANDEZ J. 1978. — Los primeros mamíferos (Notoungulata, Henricosborniidae) de la

Formación Mealla (Grupo Salta, Subgrupo Santa Bárbara). Sus implicancias filogenéticas, taxonómicas y cronológicas. *Ameghiniana* 15: 366-390.

Paula Couto C. de 1952a. — Fossil mammals from the beginning of the Cenozoic in Brazil: Condylarthra, Litopterna, Xenungulata, and Astrapotheria. *Bulletin of the American Museum of Natural History* 99: 355-394. http://hdl.handle.net/2246/417

Paula Couto C. de 1952b. — Fossil mammals from the beginning of the Cenozoic in Brazil. Notoungulata. *American Museum Novitates* 1568:1-16. http://hdl.handle.net/2246/2390

Polly P. D. 2007. — Evolutionary biology: development with a bite. *Nature* 449: 413-415. https://doi.org/10.1038/449413a

Rasband W. S. 1997-2018. — ImageJ, U. S. National Institutes of Health, Bethesda, Maryland, United States. https://imagej.nih.gov/ij/

Rose K. D., Holbrook L. T., Rana R. S., Kumar K., Jones K. E., Ahrens H. E., Missiaen P., Sahni A. & Smith T. 2014. — Early Eocene fossils suggest that the mammalian order Perissodactyla originated in India. *Nature Communication* 5: 1-9. https://doi.org/10.1038/ncomms6570

Shelley S. L., Williamson T. E. & Brusatte S. L. 2018. — The osteology of *Periptychus* carinidens: A robust, ungulate-like placental mammal (Mammalia: Periptychidae) from the Paleocene of North America. *PLoS ONE* 13 (7): e0200132. https://doi.org/10.1371/journal.pone.0200132

Simpson G. G. 1948. — The beginning of the age of mammals in South America. Part II. *Bulletin of the American Museum of Natural History* 91 (1): 1-232. http://hdl.handle.net/2246/1632

Sprain C. J., Renne P. R., Wilson G. P. & Clemens W. A. 2015. — High-resolution chronostratigraphy of the terrestrial Cretaceous-Paleogene transition and recovery interval in the Hell Creek region, Montana. *Geological Society of America Bulletin* 127 (3-4): 393-409. https://doi.org/10.1130/B31076.1

Soria M. F. 1987. — Estudio sobre los Astrapotheria (Mammalia) del Paleoceno y Eoceno. Parte I: Descripción de *Eoastrapostylops riolorense* Soria y Powell, 1982. *Ameghiniana* 24: 43-51.

Soria M. F. & Powell J. E. 1981. — Un primitivo Astrapotheria (Mammalia) y la edad de la Formación Río Loro, Provincia de Tucumán, República Argentina. *Ameghiniana* 18:155-168.

Stehlin H. G. 1916. — Die Säugetiere des schweizerischen Eocaens. Critischer Catalog der materialien. *Caenopithecus – Necrolemur – Microchoerus – Nannopithex – Anchomomys – Periconodon – Amphichiromys – Heterochiromys* – Nachträge zu *Adapis* – Schlussbetrachtungen zu den Primaten. *Abhandlungen Schweizerischen Paläontologischen Gesellschaft* 41: 1299-1552. https://biodiversitylibrary.org/page/14836550

Thenius E. 1989. — Zähne und Gebiß der Säugetiere, *in* Niethammer J., Schliemann H., & Starck D. (eds), *Handbook of Zoology.* Volume 8. *Mammalia*, part 56. Walter de Gruyter, Berlin: 1-513.

Thewissen J. G. M., Russell D. E., Gingerich P. D. & Hussain S. T. 1983. — A new dichobunid artiodactyl (Mammalia) from the Eocene of north-west Pakistan. *Proceedings of the Koninklijke Nederlandse Akademie van Wetenschappen, Series B*, 86 (2): 153-180.

Voruz C. 1970. — Origine des dents bilophodontes des Cercopithecoidea. *Mammalia* 34 (2): 269-293. https://doi.org/10.1515/mamm.1970.34.2.269

Welker F., Collins M. J., Thomas J. A., Wadsley M., Brace S. & Cappellini E., Turvey S. T., Reguero M., Gelfo J. N., Kramarz A., Burger J., Thomas-Oates J., Ashford D. A., Ashton P. D., Rowsell K., Porter D. M., Kessler B., Fischer R., Baessmann C., Kaspar S., Olsen J. V., Kiley P., Elliott J. A., Kelstrup C. D., Mullin V., Hofreiter M., Willerslev E., Hublin J.-J., Orlando L., Barnes I. & MacPhee R. D. E. 2015. — Ancient proteins resolve the evolutionary history of Darwin's South American ungulates. *Nature* 522: 81-84. https://doi.org/10.1038/nature14249

Westbury M., Baleka S., Barlow A., Hartmann S., Paijmans J. L. A., Kramarz A., Forasiepi A. M., Bond M., Gelfo J. N., Reguero M. A., Lopez Mendoza P., Taglioretti M., Scaglia F, Rinderknecht A., Jones W., Aguilar J. L., Billet G., Muizon C. de, MacPhee R. D. E. & Hofreiter M. 2017. — A mitogenomic timetree for Darwin's "transitional" South American mammal, *Macrauchenia patachonica*. *Nature Communications* 8: 15951. https://doi.org/10.1038/ncomms15951

Wheeler W. H. 1961. — Revision of the Uintatheres. *Peobody Museum of Natural History*, *Bulletin* 14: 1-93. https://biodiversitylibrary.org/page/10600608

Wible J. R., Novacek M. J. & Rougier G. W. 2004. — New data on the skull and dentition in the Mongolian Cretaceous eutherian mammal *Zalambdalestes*. *Bulletin of the American Museum of Natural History* 281: 1-144. https://doi.org/10.1206/0003-0090(2004)281<0001:NDOTSA>2.0.CO;2

Wible J. R., Rougier G. W., Novacek M. J. & Asher R. J. 2009. — The eutherian mammal *Maelestes gobiensis* from the Late Cretaceous of Mongolia and the phylogeny of Cretaceous Eutheria. *Bulletin of the American Museum of Natural History* 327: 1-123. https://doi.org/10.1206/623.1

Williamson T. E., Weil A. & Standhardt B. 2011. — Cimolestids (Mammalia) from the early Paleocene (Puercan) of New Mexico. *Journal of Vertebrate Paleontology* 31: 162-180. https://doi.org/10.1080/02724634.2011.539649

Wilson G. P. 2013. — Mammals across the K/Pg boundary in Northeastern Montana, USA: Dental morphology and body-size patterns reveal extinction selectivity and immigrant-fueled ecospace filling. *Paleobiology* 39: 429-469. https://doi.org/10.1666/12041

Wilson G. P. 2014. — Mammalian extinction, survival, and recovery dynamics across the Cretaceous-Paleogene boundary in Northeastern Montana, USA, *in* Wilson G. P., Clemens W. A., Horner J. R., & Hartman J. H. (eds), *Through the End of the Cretaceous in the Type Locality of the Hell Creek Formation in Montana and Adjacent Areas*. Geological Society of America, Special Paper 503: 365-392. https://doi.org/10.1130/2014.2503(15)

Wilson L. A., Sánchez-Villagra M. R., Madden R. H. & Kay R. F. 2012. — Testing a developmental model in the fossil record: molar proportions in South American ungulates. *Paleobiology*, 38 (2): 308-321. https://doi.org/10.1666/11001.1

Woodburne M. O., Goin F. J., Bond M., Carlini A. A., Gelfo J. N., Lopez G. M., Iglesias A. & Zimicz A. N. 2014a. — Paleogene land mammal faunas of South America; a response to climatic changes and indigenous floral diversity. *Journal of mammalian Evolution* 21 (1): 1-73. https://doi.org/10.1007/s10914-012-9222-1

Woodburne M. O., Goin F. J., Raigemborn M. S., Heizler M., Gelfo J. N. & Oliveira E. V. 2014b. — Revised timing of the South American Early Paleogene land mammal ages. *Journal of South American Earth Sciences* 54: 109-119. https://doi.org/10.1016/j.jsames.2014.05.003

Submitted on 26 February 2019;
accepted on 27 June 2019;
published on 19 December 2019.

APPENDIX 1. — Comparison taxon list, specimens and references.

Taxa, specimens and references concerning the section "Molar proportions in kollpaniines and other 'ungulates'" are indicated in Table 8.

Alcidedorbignya inopinata MHNC 8372, 8399; Muizon & Marshall (1987); Muizon *et al.* (2015);
Asioryctes and *Kennalestes* (Kielan-Jaworowska 1981; Wible *et al.* 2004);
Asmithwoodwardia scotti, DGM 358-M; Paula Couto (1952a);
Aspanlestes aptap, Nessov *et al.* (1998), Archibald & Averianov (2005);
Baioconodon nordicum, cast of YPM-PU 14234;
Colbertia magellanica, cast of DGM 357-M; Paula-Couto (1952b);
Didolodus multicuspis, MACN 10690;
Eoastrapostylops riolorense, Soria & Powell (1981), Soria (1987);
Ernestokokenia cf. nitida, MNHN.F.CAS681, Muizon & Cifelli (2000);
Escribania chubutensis, cast of (MLP 90-II-12-63), Gelfo *et al.* (2007);
Hallensia louisis, Hooker (1994);
Henricosbornia lophodonta, MACN 10808;
cf. *Henricosbornia*, MNHN.F.CAS2714;
Hyracotherium, Hooker (1994);
Kulbeckia kulbecke, Wible *et al.* (2004, 2009);
Lamegoia conodonta, casts of MNRJ 1463-V, MNRJ 1465-V, MNRJ 1464-V (specimen referred by Paula Couto [1952a] to *Lamegoia conodonta* but referred in this paper to a large didolodontid close to *Ricardocifellia*);
Maiorana noctiluca, cast of YPM-PU 16667 and 14171;
Miguelsoria parayirunhor, cast of MNRJ 4094-V; Cifelli (1983);
Oxyprimus galadrielae (cast of YPM-PU 21015);
Parazhelestes robustus (Nessov *et al.* 1998; Archibald & Averianov 2005);
Pascualodus patagoniensis cast of MLP59-II-24-39, Gelfo (2004);
Pliolophus quesnoyensis, MNHN.F.QNY2-2811, QNY1-482, QNY2-2880, QNY1-519, QNY2-2883, QNY2-2903, QNY2-2700, QNY2-2867, QNY2-2869, QNY1-382, QNY2-2900, QNY2-2705, QNY2-2854, QNY2-2707, QNY2-2815, QNY2-2808; Bronnert *et al.* (2017);
Prokennalestes trofomovi and *P. minor*, Kielan-Jaworowska & Dashzeveg (1989);
Promioclaenus acolytus, USNM 9575, AMNH 32728;
Promioclaenus lemuroides, AMNH 4025;
Propachynolophus levei, Hooker (1994);
Protolipterna ellipsodontoides, MCT-1495M;
Puercolestes simpsoni, Williamson *et al.* (2011);
Raulvaccia peligrensis, cast of MLP 90-II-12-70; Gelfo (2007);
Ricardocifellia protocenica, cast of DGM 908M, MNRJ 1462-V; Paula Couto (1952a), Cifelli (1983);
Simpsonotus praecursor cast of MLP 73-VII-3-11; Pascual *et al.* (1978);
Zalambdalestes, Wible *et al.* (2004).

APPENDIX 2. — List of genus and species names cited in the text with authorship and year.

Alcidedorbignya Muizon & Marshall, 1987;
Alcidedorbignya inopinata Muizon & Marshall, 1987;
Asioryctes Kielan-Jaworowska, 1975;
Asmithwoodwardia Ameghino, 1901;
Asmithwoodwardia scotti Paula Couto, 1952;
Aspanlestes Nessov, 1985;
Aspanlestes aptap Nessov, 1985;
Baioconodon Gazin, 1941;
Baioconodon nordicum (Jepsen, 1930);
Colbertia Paula Couto, 1952;
Colbertia magellanica Price & Paula Couto, 1950;
Didolodus Ameghino, 1897;
Didolodus multicuspis Ameghino, 1897;
Eoastrapostylops Soria & Powell, 1981;
Eoastrapostylops riolorense Soria & Powell, 1981;
Ernestokokenia Ameghino, 1901;
Ernestokokenia nítida Ameghino, 1911;
Escribania Bonaparte Van Valen & Kramartz, 1993;
Escribania chubutensis Van Valen & Kramartz, 1993;
Hallensia Franzen & Haubold, 1986;
Hallensia louisi Hooker, 1994;
Henricosbornia Ameghino, 1901;
Henricosbornia lophodonta Ameghino, 1901;
Hyracotheriumi Owen, 1841;
Kennalestes Kielan-Jaworowska, 1968;
Kulbeckia Nessov, 1993;
Kulbeckia kulbecke Nessov, 1993;
Lamegoia Paula Couto, 1952;
Lamegoia conodonta Paula Couto, 1952;
Licaphrium Ameghino, 1887;
Maiorana Van Valen, 1978;
Maiorana noctiluca Van Valen, 1978;
Miguelsoria Cifelli, 1983;
Miguelsoria parayirunhor (Paula Couto, 1952);
Oxyprimus Van Valen, 1978;
Oxyprimus galadrielae Van Valen, 1978;
Parazhelestes Nessov, 1993;
Parazhelestes robustus Nessov, 1993;
Pascualodus Gelfo, 2004;
Pascualodus patagoniensis Gelfo, 2004;
Picturotherium Kramartz & Bond, 2005;
Pliolophus Owen, 1858;
Pliolophus quesnoyensis Bronnert, Gheerbrant, Godinot & Métais, 2017;
Prokennalestes Kielan-Jaworowska & Dashzeveg, 1989;
Prokennalestes trofimovi Kielan-Jaworowska & Dashzeveg, 1989;
P. minor Kielan-Jaworowska & Dashzeveg, 1989;
Promioclaenus Trouessart, 1904;
Promioclaenus acolytus Cope, 1882;
P. lemuroides (Matthew, 1897);
Propachynolophus Pomel, 1847;
Propachynolophus levei Hooker, 1994;
Protolipterna Cifelli, 1983;
Protolipterna ellipsodontoides Cifelli, 1983;
Puercolestes Reynolds, 1936;
Puercolestes simpsoni Reynolds, 1936;
Raulvaccia Van Valen & Kramartz, 1993;
Raulvaccia peligrensis Van Valen & Kramartz, 1993;
Ricardocifellia Mones, 2015;
Ricardocifellia protocenica: Paula Couto (1952);
Simpsonotus Pascual Vucetich & Fernandez, 1978;
Simpsonotus praecursor Pascual, Vucetich & Fernandez, 1978;
Zalambdalestes Kielan-Jaworowska, 1981.